DOCTORAL DISSERTATION

Study on relationship between CH_4 flux and wetting at taiga-tundra boundary in northeastern Siberia using stable isotope ratios of CH_4

北東シベリアタイガ - ツンドラ境界域における

湿潤化前後の CH_4 フラックスと CH_4 安定同位体比の利用

Division of Earth System Science,

Graduate School of Environmental Science,

Hokkaido University

北海道大学大学院環境科学院地球圏科学専攻

Ryo SHINGUBARA

新宮原　諒

February 2019

Abstract

Methane is one of the important greenhouse gases. Methane emission from natural wetlands is the largest individual source of the atmospheric CH_4. The size of this source depends on meteorological conditions such as precipitation, and a significant driver of the interannual variations in the global CH_4 source. Higher water level in wetlands and terrestrial ecosystems generally leads to higher CH_4 emission in spatial variation. On the contrary, the temporal variation in the CH_4 emission tends to be more complicated. Flooding can increase CH_4 emission after a time lag. Higher water level can also occur with lower CH_4 emission. To understand the relationship between wetting and CH_4 emission, it is necessary to assess the underlying processes, CH_4 production, oxidation and transport, which are reflected in stable isotope ratios of CH_4.

Taiga-tundra boundary ecosystem on the Indigirka River lowlands in northeastern Siberia has a gradient in soil wetness conditions, corresponding to the microtopography. Higher micro-relief in the ground level is drier and covered by green mosses, larch trees and shrubs (termed “tree mound”). Lower micro-relief is wetter and covered by wetland vegetation, such as sphagnum mosses and sedges (“wet area”). Thus, this ecosystem was assumed to have micro-reliefs in the gradient with large interannual

variations in soil wetness conditions. Actually, the ecosystem experienced a wetting event with extreme precipitation in 2011.

This study observed interannual variations in CH_4 flux and dissolved CH_4 concentration during the summer from 2009 to 2013 at the taiga-tundra boundary in the vicinity of Chokurdakh (70° 37′ N, 147° 55′ E) to investigate the relationship between CH_4 flux and wetting. The interannual flux variations were observed with portable manual chambers. As a complement, an automatic chamber system was modified to make continuous observations of CH_4 flux. In order to assess variations in CH_4 production and oxidation processes after the wetting event, $\delta^{13}C$ and δD of dissolved CH_4 were analyzed from 2011 to 2013. In addition, soil incubation experiments were conducted under anaerobic and aerobic conditions to investigate the behaviors of $\delta^{13}C$ and δD of CH_4 with regards to CH_4 production and oxidation processes in this ecosystem.

Methane flux showed large interannual variations in wet areas (36–140 mg CH_4 m^{-2} day^{-1} emitted). Increased CH_4 emission was recorded in the summer of 2011 when a wetting event with extreme precipitation occurred. Methane emission remained relatively large in 2012, and increased further in 2013, although water level declined from 2011 to 2013. Thaw depth became deeper from 2011 to 2013, which may partly

explain the increase in CH_4 emission. Moreover, dissolved CH_4 concentration showed a sharp increase of one order of magnitude from 2011 to 2012 and increased further from 2012 to 2013.

Variations in individual $\delta^{13}C$ and δD values of dissolved CH_4 (10 cm depth) became smaller from 2011 to 2012 and 2013. These δ valuese clustered around the higher $\delta^{13}C$ and lower δD values, which were seen in the anaerobic incubation experiment along with high CH_4 production rates, suggesting that CH_4 production was enhanced in 2012 and 2013. In addition, the lower δD values in 2012 and 2013 suggests that CH_4 oxidation became less significant after the wetting event, based on the results of aerobic incubation experiment. These enhanced CH_4 production and less significant CH_4 oxidation, which could led to the buildup of dissolved CH_4 and the increase in CH_4 emission, may have been caused by continued soil reduction across multiple years following the wetting event. Additionally, the clustered and higher $\delta^{13}C$ values of dissolved CH_4 in 2012 and 2013 suggests that delayed activation of acetoclastic methanogenesis following the soil reduction could also have contributed to the enhancement of CH_4 production.

This study shows a multi-year effect of wetting on CH_4 emission, which suggests that duration of water saturation in the active layer can be important for predicting CH_4 emission following a wetting event in permafrost ecosystem.

Keywords: methane emission, interannual variations, carbon isotopes, hydrogen isotopes, permafrost ecosystem, Arctic

Contents

Chapter 1 General introduction

1.1 CH_4 emission from natural wetlands

Methane in the atmosphere has an important greenhouse effect (Myhre et al., 2013). Methane is exchanged between the atmosphere and the terrestrial ecosystem, especially with soil (Ciais et al., 2013). Methane is emitted from wetlands to the atmosphere, and oppositely atmospheric CH_4 is consumed by drier soil such as in forests (King, 1997; Ciais et al., 2013). In wetlands, soil organic matter is decomposed anaerobically and CH_4 is produced by a group of strictly anaerobic archaea, methanogens, as an end product of the anaerobic decomposition (Lai, 2009). In drier soil, atmospheric O_2 is provided into the soil and methanotrophic bacteria (aerobic bacteria) oxidize atmospheric CH_4 using the O_2, producing CO_2 as the end product (Conrad, 2007). In this way, the richness or poorness of water in terrestrial ecosystem determine the aerobic or anaerobic conditions in soil, and the directions of CH_4 exchange between the ecosystem and the atmosphere.

Methane emission from wetlands is the largest individual source of the atmospheric CH_4 (Ciais et al., 2013). This source is considered to be the main driver of interannual variation in global CH_4 emission, depending on meteorological conditions such as air temperature and precipitation. For instance, Dlugokencky et al. (2009)

attributed observed high growth rates in atmospheric CH_4 concentration in 2007–2008 to high CH_4 emissions from natural wetlands that resulted from anomalous high temperatures in the Arctic and greater than average precipitation in the tropics. Atmospheric CH_4 has been increasing from 2007 through the present (Nisbet et al., 2014).

Methane flux from wetland soil to the atmosphere (I define a positive flux value as CH_4 emissions) is determined by three processes: CH_4 production, oxidation, and transport (Lai, 2009). Methane is produced by strictly anaerobic *Archaea* (methanogens) mainly via hydrogenotrophic methanogenesis ($4H_2+CO_2 \rightarrow CH_4+2H_2O$) or acetoclastic methanogenesis ($CH_3COOH \rightarrow CH_4+CO_2$) as an end product of organic matter decomposition (Lai, 2009). In the soil's aerobic zone, CH_4 is oxidized to CO_2 by methanotrophic bacteria utilizing O_2, which reduces CH_4 emission to the atmosphere (Lai, 2009). Underground CH_4 is transported to the atmosphere via bubble ebullition, diffusion through soil layers and surface water, and via aerenchyma of vascular plants (Lai, 2009).

1.2 CH_4 flux and wetting

High water levels can lead to development of reducing conditions in soil, which can

promote CH_4 production or depress CH_4 oxidation, both leading to increases in CH_4 flux (Lai, 2009). This is reflected in the widely observed positive relationship between water level and CH_4 flux, found in a meta-analysis across the circum-Arctic permafrost zone (Olefeldt et al., 2013). Meanwhile, Desyatkin et al. (2014) observed increases in CH_4 flux during the second consecutive year of flooding at a thermokarst depression in boreal eastern Siberia. Treat et al. (2007) reported observations at a temperate fen in the northeastern USA, showing that high water level coincided with high CH_4 flux in interannual variations. However, water level correlated negatively with CH_4 flux over shorter timescales, namely as monthly means or individual measurements. These observational results imply that wetting is not directly related to CH_4 flux in wetlands. To understand the relationship between wetting and CH_4 flux, it is necessary to assess the underlying processes.

1.3 Stable isotope ratios of CH_4

Stable isotopes of CH_4 have been used to estimate production pathways of CH_4 (Sugimoto and Wada, 1993, 1995; McCalley et al., 2014; Itoh et al., 2015), determine the fraction of oxidized CH_4 versus produced CH_4 (Marik et al., 2002; Preuss et al., 2013), and study mechanisms of CH_4 transport by plants (Chanton, 2005).

When CH_4 in soil is lost by oxidation or diffusion, both $\delta^{13}C$ and δD of the remaining CH_4 increase. While the hydrogen isotope ratio increases more than that of carbon during oxidation, both ratios are considered to change to the same extent during diffusion. Thus it is useful to analyze both carbon and hydrogen isotopes of CH_4 to distinguish the effects of both of these processes (Chanton, 2005).

1.4 Taiga-tundra boundary ecosystem

The taiga–tundra boundary ecosystem (or transition zone) contains vegetation types of both taiga and tundra ecosystems. Liang et al. (2014) reported that the distribution of vegetation types at the taiga–tundra boundary on the lowland of the Indigirka River in northeastern Siberia is controlled by soil moisture, which corresponds to microtopography. Larches, the dominant tree species in the taiga forests of eastern Siberia, grow on microreliefs with higher ground level and drier soil, while wetland vegetation such as sphagnum mosses and sedges, typically seen in wet tundra (van Huissteden et al., 2005, 2009; van der Molen et al., 2007), dominates lower and wetter microreliefs. Thus, it is reasonable to assume that the taiga–tundra boundary ecosystem has various microreliefs in terms of interannual variation in soil wetness conditions: always wet microreliefs, always dry microreliefs, and microreliefs with

large interannual wetness variations. Hence, this ecosystem is a suitable area to evaluate the processes controlling CH_4 flux in relation to soil wetting and/or drying on an interannual timescale.

1.5 Research aim

In this study, to understand relationships between CH_4 flux and environmental factors, I observed interannual variations in chamber CH_4 flux, along with the concentration, $\delta^{13}C$, and δD of dissolved CH_4 during the summer, from 2009 to 2013, at the taiga–tundra boundary located on Indigirka River lowlands in northeastern Siberia. I also conducted soil incubation experiments to investigate how δ values of CH_4 reflect CH_4 production and oxidation processes in this ecosystem. In 2011, a wetting event with a significant amount of precipitation occurred. I focused in particular on the responses of CH_4 flux and other underlying processes to this unusual wetting event.

Chapter 2 Methods

2.1 Study sites

The taiga–tundra boundary on the lowlands of the Indigirka River was selected as our study area. Observations and sampling were conducted at three sites (V: Verkhny Khatistakha; K: Kodac; B: Boydom) in the vicinity of Chokurdakh (70°37′ N, 147°55′ E), Republic of Sakha (Yakutia), Russia (Table 2.1 and Fig. 2.1). The sites are located in the Russian Arctic with an annual mean air temperature of −13.9 °C and an annual mean precipitation of 208 mm for the period of 1950–2008, according to the Baseline Meteorological Data in Siberia database (Yabuki et al., 2011). Sites V, K, and B are beside the Indigirka River or its tributary, and tree density decreases from site V to site B.

These study sites are underlain by continuous permafrost (Iwahana et al., 2014). Normally, snowmelt and the start of active layer thawing begin in the latter half of May through the first half of June, and the growing season occurs from the end of June through the beginning of August. Air temperature and surface soil temperature (10 cm in depth) peak in July, whereas the maximum thaw depth occurs from the latter half of August to the first half of September. The freezing of the active layer starts in the latter

half of September to October and the whole active layer freezes from November to December.

Observations of CH_4 flux were conducted at seven points with three typical vegetation types, as summarized in Table 2.1. These vegetation types are distributed in patches, corresponding to microtopography and soil moisture (Liang et al., 2014). Microrelief with a higher ground level is covered by green moss, larch trees, and shrubs of willows or dwarf birches. Conversely, lower microrelief is covered by wetland vegetation of sphagnum moss or sedges. In this study, the former vegetation type was termed "tree mound", and the latter type was termed "wet area". Observation points in tree mounds were selected at each of the sites V, K, and B and termed "tree mound_V", "tree mound_K", and "tree mound_B" (Table 2.1). For observation points of wet areas, a microrelief covered by sphagnum moss at site K was termed "sphagnum_K", and points covered by sedges including, in particular, cotton sedges (*Eriophorum angustifolium*) at sites V, K, and B were termed "sedge_V", "sedge_K", and "sedge_B", respectively. Measurements of volumetric water content in the surface soil layer (0–20 cm) by TDR (time domain reflectometry; TDR-341F, Fujiwara Scientific Company, Japan) showed that tree mounds were drier than wet areas; this will be described in Section 3.3.1 (Table 2.1).

2.2 CH_4 flux observation by portable manual chambers

Methane flux during the summer from 2009 to 2013 before and after a wetting event was observed by portable manual chambers (Fig. 2.2). A transparent cylindrical flux chamber (acrylic resin, base area 4.7×10^2 cm^2, height 25 cm) was installed on the ground. The headspace gas of the chamber (ca. 12 L) was circulated with a pump (ca. 1 L min^{-1}). The chamber was closed for 15–30 min and headspace gas was sampled two to three times after chamber closure. In most cases, the chamber was closed for 30 min and headspace gas was collected at 0, 15, and 30 min after closure. Samples were kept in pre-evacuated glass vials with butyl rubber septa. To minimize soil disturbance, we stepped on wooden boards at observation points. In 2009 and 2010, CH_4 flux measurements were conducted in the latter half of July, and from 2011 to 2013 observations were conducted continuously from early July to the end of July or early August. For all of these years, the observation period included the warmest season when CH_4 emission was expected to be the most active (Table 3.1)

Concurrently with each flux measurement, soil temperature around the flux chamber was measured with a temperature sensor in an ORP electrode (PST-2739C, DKK-TOA Corporation, Japan) with an ORP meter (RM-30P or RM-20P). After flux

measurement samples were collected, thaw depth was observed on the same day around each chamber by inserting a steel rod into the ground. From 2011 on, water level was also measured after flux measurements around each chamber in wet areas using a scale. The water level was expressed as height relative to the ground surface or the moss surface. Observation dates of these environmental factors are shown in Table 3.1.

2.3 Sampling of dissolved CH_4 in situ

For measurements of dissolved CH_4, surface water and soil pore water were sampled in wet areas from 2011 to 2013. Surface water was directly taken up by a 50 mL plastic syringe with a three-way cock attached to its tip, whereas soil pore water was sampled by a 50 mL syringe (with a three-way cock attached) through a plastic tube inserted in the soil. Soon after collecting water samples, dissolved CH_4 was extracted inside the syringes with the headspace method, after adding 15–35 mL of the atmosphere prepared in a 10 L aluminum bag. This atmosphere was collected beforehand at Chokurdakh village or our observation sites and filtered using Molecular Sieves 5Å (1⁄16 pellets, FUJIFILM Wako Pure Chemical Corporation, Japan). The atmosphere was analyzed later for CH_4 concentration and isotopic compositions as a background sample (2.0–4.3 ppm for CH_4 concentration, −53 ‰ to −45 ‰ for $\delta^{13}C$ of CH_4,

and −168 ‰ to −78 ‰ for δD of CH_4). The syringes were vigorously shaken for 1 min and left standing for 5 min to ensure equilibration. Finally, headspace gas in the syringes was preserved in 10–20 mL pre-evacuated glass vials with rubber septa.

2.4 Sample analysis of CH_4 concentration and data processing

Methane concentrations in air samples from flux observation (Section 2.2) and in those from extraction of dissolved CH_4 samples (Section 2.3) were analyzed using a gas chromatograph (HP6890 series G1530A, Hewlett Packard, USA) equipped with a flame ionization detector and a CP-carboPLOT capillary column (Varian, USA). Methane flux was calculated from CH_4 concentration in chamber headspace by a linear regression of two to three concentration values against the time elapsed since chamber closure. The detection limit of CH_4 flux for each observation was calculated as 0.8–2.4 mg CH_4 m^{-2} day^{-1}, based on whether the change of chamber CH_4 concentration during the observation was significant relative to the precision of CH_4 concentration analysis. Regression r^2 was calculated (formally) as ≥0.87, when the flux value was larger than 2 mg CH_4 m^{-2} day^{-1}.

Dissolved CH_4 concentrations were obtained from calculation of the headspace method for which equilibrations of CH_4 between gas and water phases are described by

the Bunsen absorption coefficient of CH_4 (Yamamoto et al., 1976). When calculating $\delta^{13}C$ and δD of dissolved CH_4, the effect of CH_4 in background air was removed based on the mass balance.

All statistical tests for detecting differences in CH_4 fluxes or dissolved CH_4 concentrations were conducted using R software (version 3.3.3). Mann–Whitney's U test was applied to compare magnitudes between 2 years of data and Steel–Dwass's multiple comparison test was used to compare magnitudes among 3 years or more of data.

2.5 Automatic chamber system

To conduct continuous observations of CH_4 flux for a whole day and from early July to late July, an automatic chamber system (made by Technical Division, Institute of Low Temperature Science, Hokkaido University) was modified and applied to site K during the summer from 2013 to 2016 (only a part of the data from 2016 will be shown in this dissertation). Originally, the automatic chamber system (Fig. 2.3) was made for observing soil respiration and includes three transparent chambers and three dark chambers. The chambers close and open their lids automatically following a program in a measurement and control data logger CR1000 (Campbell Scientific, Inc., USA)

installed in the control box of the chamber system. One chamber is closed at one time and headspace gas in the chamber is circulated between the chamber and the control box. The gas is analyzed for CO_2 concentration every 10 seconds by a CO_2 gas analyzer LI-820 (LI-COR Biosciences, Inc., USA) in the control box.

In this study, a photoacoustic field gas monitor INNOVA 1412 (LumaSense Technologies, Inc., USA) was connected to the chamber system to analyze CH_4 concentration in chamber headspace gas at the same time with the CO_2 measurement (Fig. 2.3). This gas monitor measured CH_4 concentration continuously at one time per approximately 1 min. In 2016, one chamber was programmed to be closed for 10 min in one flux measurement so that approximately 10 data points of CH_4 concentration were obtained in a flux measurement. The six automatic chambers were closed one by one for flux measurements, which comprised one measurement cycle of 60 min. This cycle was repeated for continuous observation of CH_4 flux.

Fig. 2.4 shows an example of linearity in the chamber observation and that of testing CH_4 concentration measurement by INNOVA 1412. As seen in Fig. 2.4a, CH_4 concentration in chamber headspace increased linearly against time after a chamber closure (chamber No. 1 in sedge_K on 26 July 2016), and CH_4 flux could be calculated from the slope of the regression line. In the test of INNOVA 1412 (Fig. 2.4b), CH_4

concentration of the same gas samples was analyzed by INNOVA 1412 in site K in July 2016 and on the gas chromatograph in Hokkaido University (described in Section 2.4). In a cross plot of CH_4 concentration values by INNOVA 1412 versus those by gas chromatography (Fig. 2.4b), data points were plotted on the 1:1 line. In this way, the CH_4 concentration data analyzed by INNOVA 1412 could be validated by gas chromatography.

2.6 Analysis of $\delta^{13}C$ and δD of CH_4 samples

To analyze carbon and hydrogen isotope ratios of dissolved CH_4 samples, a continuous flow system GC/GC/C/IRMS (Sugimoto, 1996) for carbon isotopes was modified and used in this study (Fig. 2.5). The modified system consisted of two gas chromatographs GC-8A (Shimadzu, Japan) and Trace GC Ultra (Thermo Fisher Scientific, USA), combustion and HTC reactors in GC IsoLink (Thermo Fisher Scientific), and an isotope ratio mass spectrometer MAT253 (Thermo Fisher Scientific). This system can analyze gas samples with CH_4 concentration from 2 ppm (atmospheric CH_4) to 100%. The accompanying components in a CH_4 sample such as N_2 and O_2 were separated by differences in retention time in the two gas chromatographs, and CH_4 was purified. For carbon isotope analysis, the CH_4 was combusted at 1030 °C by copper oxide and nickel

oxide catalysts in the combustion reactor and converted to CO_2. The catalysts were regenerated in O_2 flow at 1030 °C. For hydrogen isotope analysis, the CH_4 was pyrolyzed to H_2 in a ceramic tube (HTC reactor) at 1420 °C. The obtained CO_2 or H_2 were introduced to the mass spectrometer, and carbon and hydrogen isotopic compositions were analyzed, respectively. Carbon and hydrogen isotope ratios were represented as delta values relative to Vienna Peedee Belemnite (VPDB) and Vienna Standard Mean Ocean Water (VSMOW), respectively. The precision was ±0.2‰ for carbon analysis and ±2‰ for hydrogen, when samples of more than approximately 8.3 nmol CH_4 and 12 nmol CH_4 were used, respectively (e.g. 100 mL and 150 mL at room temperature in standard pressure with CH_4 concentration of 2 ppm, respectively).

Table 2.1. Observation points of chamber CH_4 flux. Concentration and isotopic compositions of dissolved CH_4 were also observed in the following wet areas.

Site	Landscape	Observation points and surface conditions	Dominant vegetation	Volumetric water content (%)[b]	Thaw depth (cm)[c]
V (Verkhny Khatistakha) 70° 15' N 147° 28' E	Larch forest and wetland	tree mound_V	Green moss, *Larix gmelinii*	17 ± 5 (*n* = 3)	23 ± 3 (*n* = 5)
		sedge_V (wet area)	*Carex spp.*, *Eriophorum angustifolium*	48 ± 4 (*n* = 3)	56 ± 3 (*n* = 4)
K (Kodac)[a] 70° 34' N 148° 16' E	Typical taiga-tundra boundary	tree mound_K	Green moss, *Larix gmelinii*	2.1 ± 0.6 (*n* = 4)	23 ± 4 (*n* = 9)
		sphagnum_K (wet area)	*Sphagnum squarrosum*	42 ± 5 (*n* = 6)	31 ± 8 (*n* = 15)
		sedge_K (wet area)	*Eriophorum angustifolium*	44 ± 4 (*n* = 6)	32 ± 13 (*n* = 28)
B (Boydom) 70° 38' N 148° 09' E	Low-centered polygon	tree mound_B	Green moss, *Larix gmelinii*	6 ± 2 (*n* = 5)	20 ± 4 (*n* = 8)
		sedge_B (wet area)	*Eriophorum angustifolium*	46 ± 2 (*n* = 5)	36 ± 9 (*n* = 8)

[a] Site K was previously named as Kryvaya (Iwahana et al., 2014) or Kodak (Liang et al., 2014).

[b] Observed for the surface soil layer down to 20 cm on 1 to 3 days in July 2011 at each observation point (see Table 3.2 for detailed observation dates). Standard deviations are shown.

[c] Observed from early July to early August during 2010–2013 (see Table 3.1 for the interannual variations and Table 3.2 for detailed observation dates). Standard deviations are shown.

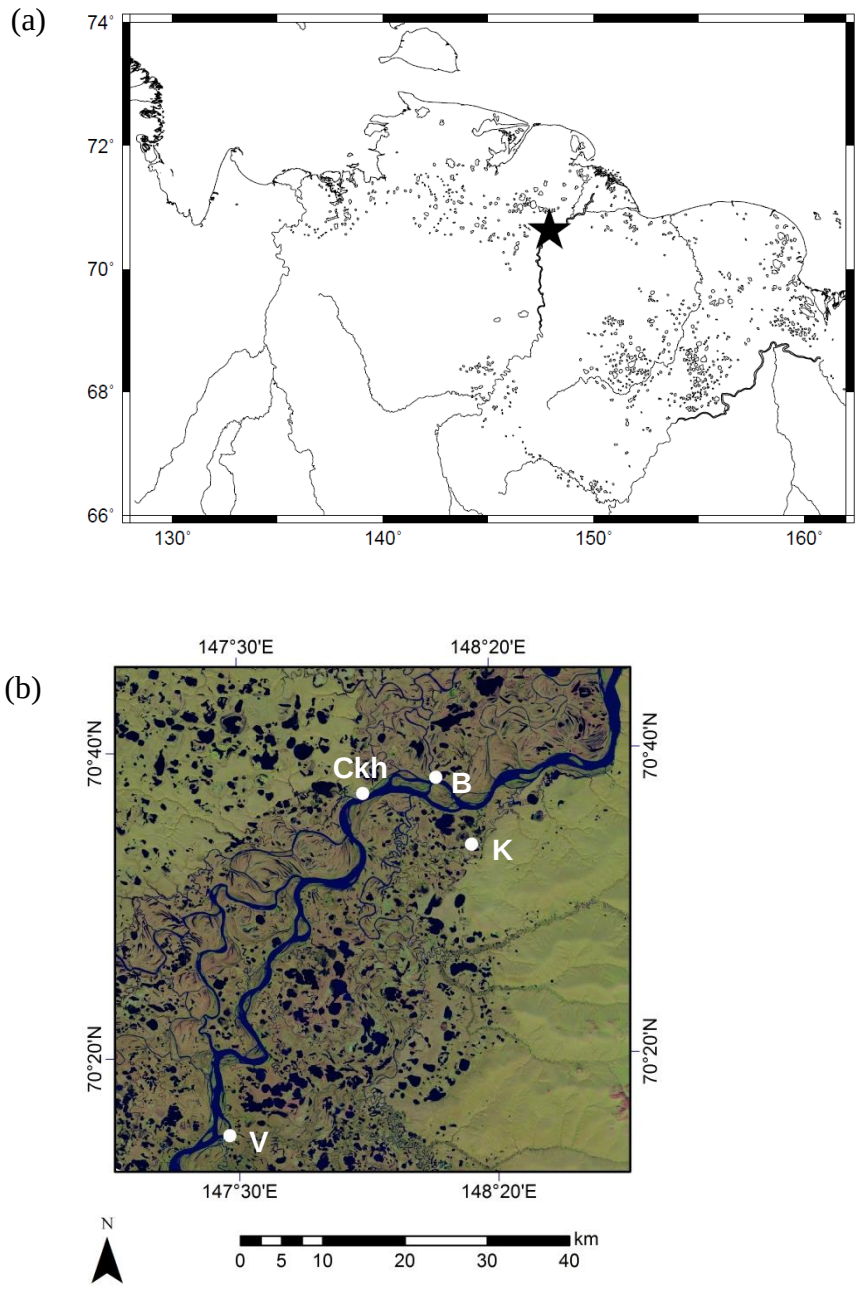

Fig. 2.1. Locations of study sites. (a) Location of study region in Northeastern Siberia (the Generic Mapping Tools 5.0.0). (b) Satellite image of Indigirka River lowland around Chokurdakh village (Ckh: 70° 37' N, 147° 55' E) from Landsat 8. Observation sites (V, K, B) were selected in this region alongside the main stem and a tributary of Indigirka River.

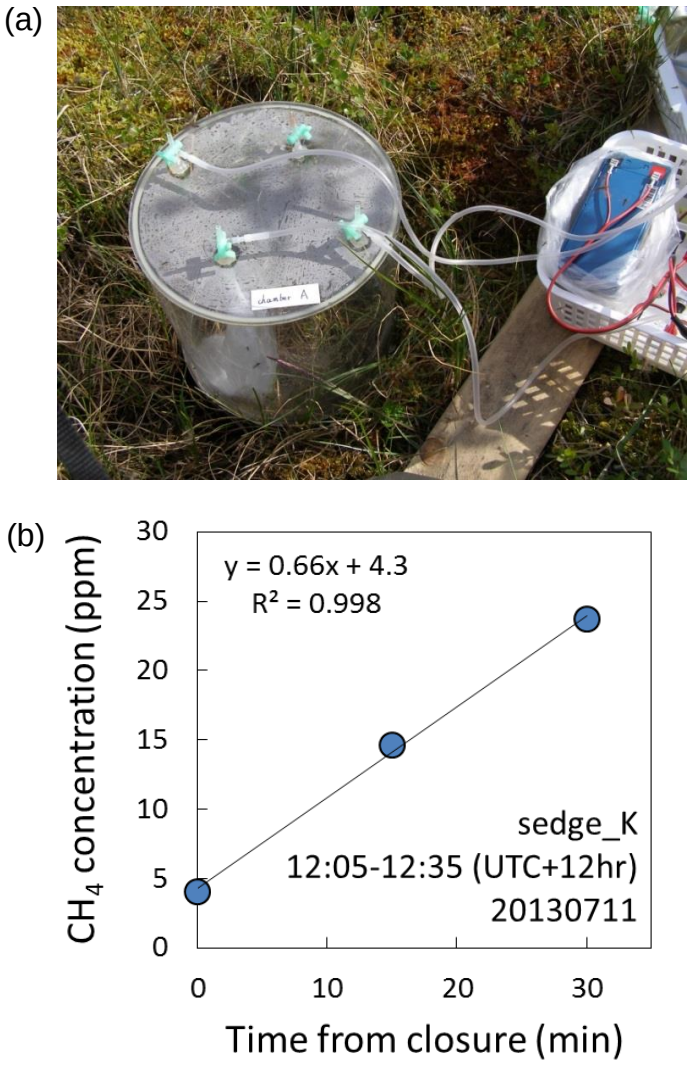

Fig. 2.2 Manual flux chamber for observing CH_4 flux before and after a wetting event. (a) Manual chamber observation. Headspace gas in the chamber was circulated through plastic tubes and a pump. (b) An example of temporal change in the CH_4 concentration in chamber headspace after chamber closure (observed in sedge_K on 11 July 2013)

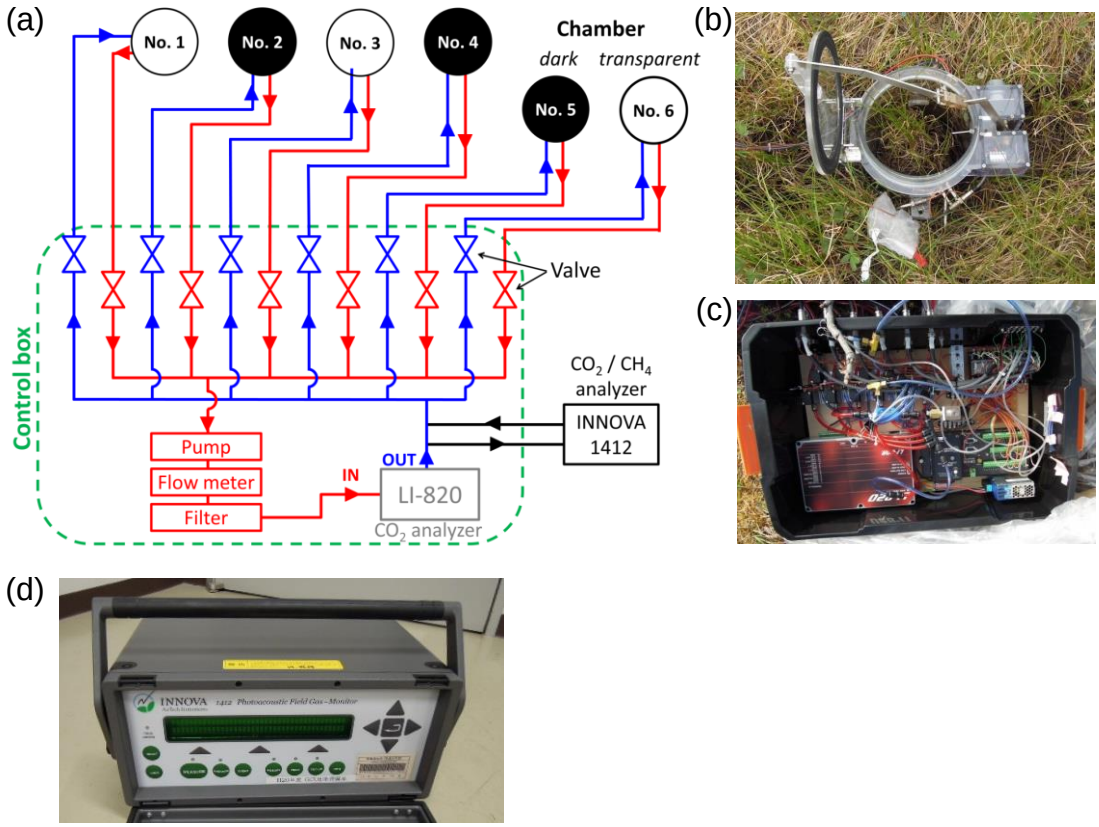

Fig. 2.3 Automatic chamber system for continuous observation of CH_4 flux. (a) Flow diagram of the system. To monitor CH_4 concentration, a photoacoustic field gas monitor INNOVA 1412 was connected to the system in parallel. (b) Automatic transparent chamber. The lid of the chamber automatically closes and opens with a motor following commands from the control box. (c) Control box of the automatic chamber system. (d) Photoacoustic field gas monitor INNOVA 1412.

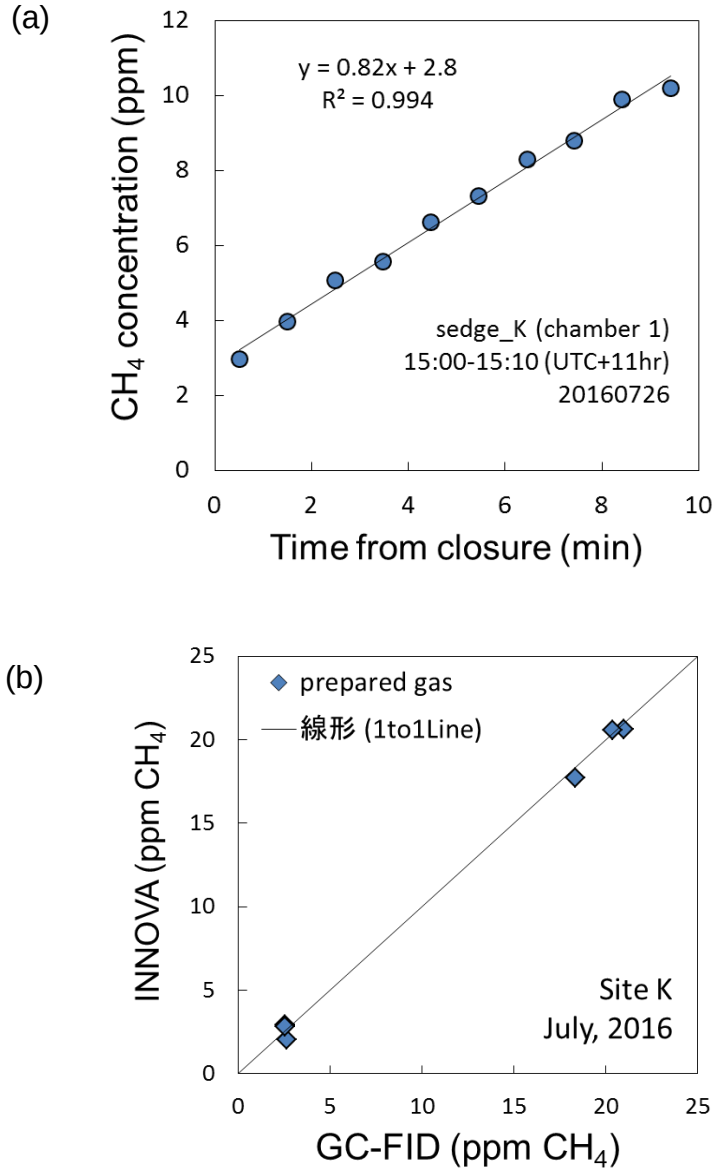

Fig. 2.4 Tests of CH_4 flux observation by the automatic chamber system. (a) An example of temporal change in the CH_4 concentration in chamber headspace after chamber closure observed in sedge_K on 26 July 2016. The CH_4 concentration increased linearly against time. (b) Comparison of CH_4 concentration values analyzed by INNOVA 1412 and gas chromatography (described in Section 2.4) of the same gas samples (in site K, July 2016). The data points were on the 1:1 line.

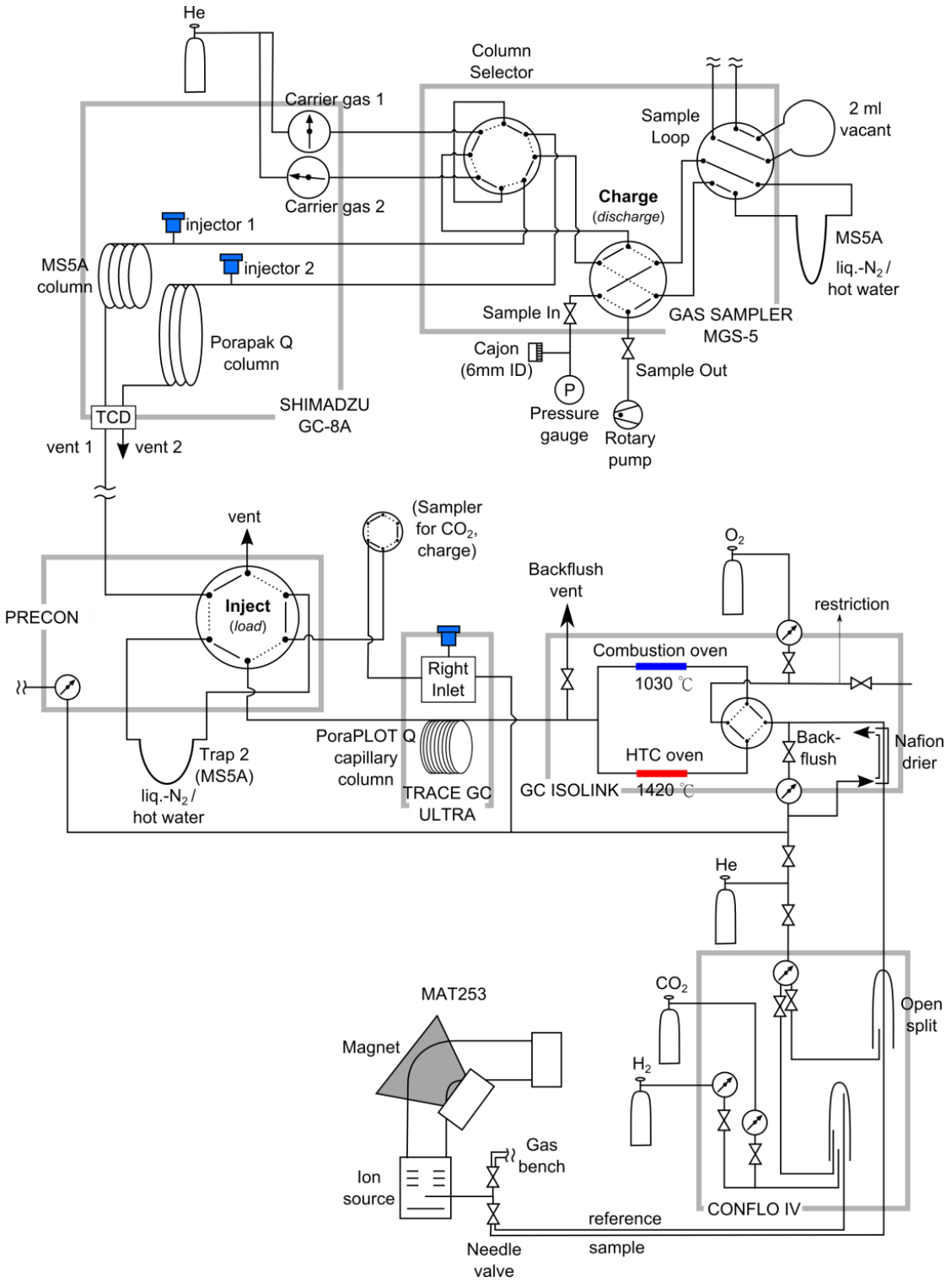

Fig. 2.5 Flow diagram of GC/GC/C(P)/IRMS, a continuous flow system for analyzing carbon and hydrogen isotopes of CH_4 samples.

Chapter 3 Interannual variations in CH_4 flux before and after a wetting event at taiga-tundra boundary in northeastern Siberia

3.1 Objective

To investigate relationship between CH_4 flux and wetting, this chapter assessed interannual variations in CH_4 flux before and after a wetting event concurrent with extreme precipitation in 2011 at taiga-tundra boundary in northeastern Siberia. Interannual variations in CH_4 flux was observed during the summer from 2009 to 2013 by portable manual chambers described in Section 2.2. Environmental factors (water level, soil temperature, and thaw depth) and dissolved CH_4 concentration in wet areas were also assessed to understand variations in CH_4 flux.

3.2 Meteorological data

Air temperature and precipitation observed at a weather station in Chokurdakh (WMO station 21946) were used to investigate interannual variations in meteorological conditions during our observation period of CH_4 flux (2009–2013) and during the preceding 2 years (2007–2008). The distance between the weather station and our farthest observation site (site V) is approximately 45 km (Fig. 2.1). These data were

obtained from GHCN-Daily, a NOAA database (Menne et al., 2012a, b).

3.3 Results

3.3.1 Environmental factors

Soil wetness conditions and thaw depth differed among vegetation types (Table 2.1). Tree mounds had lower surface water content (2.1 %–17 %) than wet areas (42 %–48 %). Among the two types of wet areas, the water level was lower in wet areas of sphagnum mosses than those of sedges (Fig. 3.1). Wet areas of sedges experienced water levels higher than the ground surface (defined as 0 cm), reaching more than 10 cm above the ground surface. Corresponding with soil water content, the thaw depth was shallower at dry tree mounds (20–23 cm) and deeper in wet areas (31–56 cm). In wet areas, thaw depth became deeper from 2011 (22±4 cm) to 2012 (25±8 cm) and 2013 (35±7 cm) in observations made during mid-July (Table 3.1). The overall average thaw depth observed on days when flux measurements were taken was 31±12 cm (n=77, 9–58 cm between 3 July and 9 August).

Figure 3.1 shows persistently low annual precipitation (162–173 mm) from 2007 to 2009. In 2010, July air temperature was characteristically high (15.5 °C) accompanying low monthly precipitation (8 mm). These show dry conditions during our

flux observations in 2009 and 2010. Parmentier et al. (2011) reported that water level was lower in summer 2009 than the previous two summers at a tundra research station (Kytalyk) in the vicinity, approximately 30 km to the northwest of Chokurdakh. In contrast, precipitation in July 2011 was extremely high (94 mm) with a relatively mild temperature (13.0 °C), which caused an unusual wetting. High precipitation continued in August (74 mm) and September (67 mm) of the same year. Corresponding with this heavy rainfall, water levels were also high in 2011, and subsequent observations show a clear decrease from 2011 to 2013 in wet areas of sedges ($p < 0.005$). Water levels also declined in wet area of sphagnum mosses, with values of −9, −10 cm, and less than −12 cm in 2011–2013.

3.3.2 CH_4 flux

Intra-diurnal variations in CH_4 flux was relatively small as seen in an example shown in Fig. 3.2 obtained by the automatic chamber system. This indicates that observation time selected in a day would not have brought biases in CH_4 flux values, although the flux measurements by portable manual chambers were conducted mainly from 11 am to 6 pm. In intra-seasonal variations in CH_4 flux observed from early July to late July in 2016 by the automatic chambers (Fig. 3.3), CH_4 flux became higher in the latter half of

July. Correspondingly, soil temperature at 10 cm depth increased later in the month. Parmentier et al. (2011) also reported a positive correlation between CH_4 flux and soil temperature at a research station (Kytalyk) of typical tundra landscape approximately 30 km to the northwest of Chokurdakh. In this study, individual flux measurements by portable manual chambers (n = 143 in total) were summarized as mean values for the main summer seasons, when CH_4 emission was expected to be the most active (Table 3.2). In 2009 and 2010, CH_4 flux was measured in the latter half of July. From 2011 to 2013, relatively continuous observations were conducted from early July to the end of July or early August in combination with dissolved CH_4 analysis, and the interannual variations during this period will be discussed in detail.

Obtained CH_4 flux shows clear spatial and interannual variations (Fig. 3.4).With regards to the spatial variation in CH_4 flux, tree mounds had consistently small values around the detection limit for all measurements (−4.9 to 1.9 mg CH_4 m^{-2} day^{-1}), while wet areas showed CH_4 emissions. From 2009 to 2013, the CH_4 flux in wet areas showed large interannual variations ranging from 36 to 140 mg CH_4 m^{-2} day^{-1}. The flux increased in 2011 when the wetting event occurred, and then remained relatively large in 2012 (compared to 2009 and 2010). Moreover, the flux increased again from 2011/2012 to 2013 ($p < 0.05$). Although water level in wet areas declined from

2011 to 2013, CH_4 flux increased from 2011/2012 to 2013 and, in 2013, became larger than the positive relationship between CH_4 flux and water level reported by Olefeldt et al. (2013) for circum-Arctic region (Fig. 3.5). No statistically significant correlation was found when CH_4 flux was plotted against soil temperature (10 cm in depth), thaw depth, or water level using all the data from wet areas (Fig. 3.6).

3.3.3 In situ dissolved CH_4 concentration

In addition to CH_4 flux, dissolved CH_4 concentration increased after the wetting event in 2011 (Fig. 3.7). From 2011 to 2012, CH_4 concentration in soil pore water at 10 cm in depth (Fig. 3.7b) exhibited a sharp increase of 1 order of magnitude ($p < 0.005$). It remained high from 2012 to 2013, and the concentrations in surface water and that at 20 cm in depth (Fig. 3.7a and c) also increased significantly over the same period ($p < 0.05$). No significant difference in concentration was observed at 30 cm in depth between 2012 and 2013. In terms of vertical variation, the concentration in surface water was lower than that in soil pore water (10, 20, and 30 cm in depth).

3.4 Discussion

3.4.1 CH_4 flux in tree mounds and wet areas in the taiga-tundra boundary on Indigirka River lowland

Methane flux observed in our study was clearly larger in wet areas than at dry tree mounds (Table 2.1, Fig. 3.4). Such differences in CH_4 flux between wetland vegetation and dry areas with trees or shrubs is generally observed (van Huissteden et al., 2005, 2009; van der Molen et al., 2007; Flessa et al., 2008) and is consistent with the fact that CH_4 production requires reducing conditions in soil (Conrad, 2007). Our CH_4 flux in wet areas (36–140 mg CH_4 m^{-2} day^{-1}) was comparable to that reported for wet tundras (32–101 mg CH_4 m^{-2} day^{-1}) or permafrost fens (42–147 mg CH_4 m^{-2} day^{-1}) in a database across permafrost zones compiled by Olefeldt et al. (2013). In forests, many studies have observed CH_4 absorption instead of emission (King, 1997; Dutaur and Verchot, 2007; Flessa et al., 2008; Morishita et al., 2014). However, our observations at tree mounds rarely found CH_4 absorption or emission. In addition, CH_4 was not consumed even under O_2- and CH_4-rich conditions in incubation experiments of tree mound soil from site K (Murase et al., 2014), indicating that a lack of methanotrophic bacterial activity limited CH_4 absorption at this vegetation type. Our results show that CH_4 emission from wet areas is expected to make a greater contribution to

ecosystem-scale CH_4 exchange at the taiga–tundra boundary on the Indigirka River lowlands.

3.4.2 Reason for the interannual variations in CH_4 flux after the wetting event

In 2009 and 2010 the CH_4 emission in wet areas was low (Fig. 3.4), even at relatively high soil temperature in 2010 (Fig. 3.6), under dry conditions that were not directly observed in this study. The wetting event in 2011 initiated the high CH_4 emission that continued through 2013 despite decreasing water levels (Fig. 3.1). Moreover, a further increase in CH_4 flux was observed in 2013, accompanying a buildup of dissolved CH_4 (2011–2013) as shown in Fig. 3.7.

These interannual variations from 2011 to 2013 could be caused by the development of reducing soil conditions over multiple years after the wetting event. Reducing soil conditions may have developed, to some extent, as a result of the extreme precipitation in the summer of 2011 (Fig. 3.1). The surface soil layer, particularly under high water levels, could eliminate O_2 from soil pore spaces due to water saturation. These reducing conditions may have been preserved by freezing of the soil throughout the following winter. Additionally, a surface soil layer saturated with ice could have prevented snowmelt water (rich in O_2) from infiltrating the soil during the spring thaw

season of 2012 (Woo, 2012). These processes would have led to the continuation of reducing conditions in the soil, which were created in summer 2011, into 2012. Through further decomposition of soil organic matter with the consumption of O_2, reducing soil conditions may have been exacerbated in the water-saturated soil layer to a greater extent in summer 2012. Water in the saturated soil layer may be retained without exchange for a relatively long time at our study sites because lateral runoff is assumed to be small in the flat floodplain that comprises the Indigirka River lowlands (Nassif and Wilson, 1975). In addition, deep percolation loss is prevented by the impermeable permafrost layer (Woo, 2012). From summer 2012 to summer 2013, reducing conditions in the soil may have been similarly prolonged, especially in the deep soil layer, despite the decrease in water level from summer 2011 to summer 2013. This continuous soil reduction from 2011 to 2013 could have promoted CH_4 production and/or decreased CH_4 oxidation, which may explain the increase in dissolved CH_4 concentration and CH_4 flux in wet areas following the wetting event and continuing until 2013 (Figs. 3.4 and 3.7).

In 2012 and 2013, we observed redox potential values lower than −100 mV in wet areas (Table 3.3), which are well below the upper limit for CH_4 production in soil (Conrad, 2007; Street et al., 2016). Methane production at a potential higher

than −100 mV can also occur because soil is heterogeneous and can have more reducing microsites than the rest of the bulk soil, where redox potential can be measured (Teh et al., 2005; Teh and Silver, 2006).

In addition to the multi-year soil reduction, it appears that the wetting event led to the thaw depth increase in wet areas from 2011 to 2013 (Table 3.1). Although thaw depth increased, summer air temperatures decreased from 2011 (7.7 and 13.0 °C as June and July mean temperatures, respectively) to 2012 (7.4, 9.2 °C) and 2013 (6.6, 10.5 °C) as shown in Fig. 3.1. The wetting event may have led to the CH_4 flux increase from 2011 to 2013 (Fig. 3.4) partly through the thaw depth increase, by thickening the soil layer where CH_4 production occurs (Nakano et al., 2000; van Huissteden et al., 2005, 2009). However, the clear increase in dissolved CH_4 concentration (Fig. 3.7) cannot be explained by the thaw depth increase.

This study did not evaluate vegetation cover quantitatively, and the wetting event might have also led to some vegetation change (such as increase in sedges), although no drastic changes were found visually in the observed wet areas. Increase in cover by sedges might have raised CH_4 flux partly by providing labile organic substrate for CH_4 production or conduits for the CH_4 transport from the soil to the atmosphere (Chanton, 2005; Lai, 2009; Ström et al., 2015).

Table 3.1. Thaw depths in tree mound and wet area observed along with CH_4 flux from 2010 to 2013. Averaged values and ranges are shown for each vegetation type and each year. Standard deviations are represented when $n \geq 3$. See Table 3.2 for each observation date.

Year	Thaw depth (cm)			
	Tree mound		Wet area	
	Mean	Range	Mean	Range
2010	23	21–25	30	29–30
	(*n* = 2)	(Jul 20–21)	(*n* = 2)	(Jul 20–21)
2011	23 ± 6	14–30	22 ± 4	15–28
	(*n* = 6)	(Jul 9–30)	(*n* = 9)	(Jul 9–21)
2012	21 ± 4	16–27	35 ± 14	9–57
	(*n* = 11)	(Jul 3 – Aug 9)	(*n* = 24)[a]	(Jul 3 – Aug 9)[a]
2013	20 ± 3	18–23	40 ± 9	23–58
	(*n* = 3)	(Jul 15 – Aug 2)	(*n* = 20)[b]	(Jul 11 – Aug 2)[b]

a During Jul 8–20, 2012 in wet area, the mean value was 25 ± 8 cm, and the range was 9–37 cm.

b During Jul 11–18, 2013 in wet area, the mean value was 35 ± 7 cm, and the range was 23–46 cm.

Table 3.2. Averaged CH_4 flux (in mg CH_4 m^{-2} day^{-1}) over each observation point and each year (2009–2013). Standard deviations are shown in case of $n \geq 3$. Dates of the flux observation are indicated in parenthesis. Superscripts represent observed environmental variables on each day: a) soil temperature (2009–2013), b) thaw depth (2010–2013), c) water level (2011–2013), and d) volumetric water content in surface soil (2011).

Observation points	Year				
	2009	2010	2011	2012	2013
tree mound_V	–	0 (Jul 16)	−1 ± 2 (Jul 23[b], 29[abd])	0 (Aug 7[ab])	0 (Aug 2[ab])
sedge_V (wet area)	3 ± 3 (Jul 23)	2 (Jul 16[a])	179 ± 66 (Jul 23[c], 29[acd])	46 (Aug 7[abc])	106 ± 21 (Aug 2[abc])
tree mound_K	0 (Jul 22)	−1 ± 3 (Jul 21[ab])	0 (Jul 15[bd], 18[bd])	0 (Jul 3[ab], 8[a], 12[ab], 24[ab]; Aug 2[ab], 6[ab])	1 (Jul 15[ab])
sphagnum_K (wet area)	–	1 ± 1 (Jul 21[ab])	43 ± 31 (Jul 11[bd], 17[b], 18[bcd], 21[bcd])	3 ± 3 (Jul 3[abc], 8[abc],12[abc], 24[abc]; Aug 2[abc], 6[abc])	102 ± 4 (Jul 11[ab], 18[ab], 25[ab], 31[ab])
sedge_K (wet area)	26 ± 24 (Jul 22[a])	–	28 ± 4 (Jul 11[bcd], 17[bc], 18[bcd], 21[abcd])	83 ± 30 (Jul 3[abc], 8[abc], 12[abc],20[abc], 21[a], 24[abc]; Aug 2[abc], 6[abc])	111 ± 63 (Jul 11[abc], 18[abc], 25[abc], 31[abc])
tree mound_B	–	0 (Jul 20[b])	0 (Jul 9[bd], 30[bd])	−1 ± 1 (Jul 13[ab], Aug 9[ab])	0 (Jul 16[ab])
sedge_B (wet area)	79 ± 80 (Jul 25)	98 ± 84 (Jul 20[b])	151 ± 58 (Jul 9[bcd], 30[acd])	131 ± 58 (Jul 13[ab], Aug 9[abc])	286 ± 49 (Jul 16[abc])

Table 3.3. Redox potential observed in summers 2012 and 2013 by ORP meter (RM-20P or RM-30P, DKK-TOA Corporation, Japan) connected with an ORP electrode (PST-2739C). Measurement accuracy of the ORP meter is ±10 mV. Redox potential value was accepted when the potential stabilized after installing the ORP electrode into the soil.

Observation points	Depth (cm)	Redox potential (mV versus the normal hydrogen electrode)	
		2012	2013
tree mound_K	10	608 to 643	478 to 482
	20	627 to 631	—
sphagnum_K (wet area)	10	−183 to 814	547 to 617
	20	−129	—
sedge_K (wet area)	10	−177 to −121	−114 to −69
	20	−250 to −78	−223 to −194
	30	−152 to −118	—
sedge_B (wet area)	10	—	−113 to −102

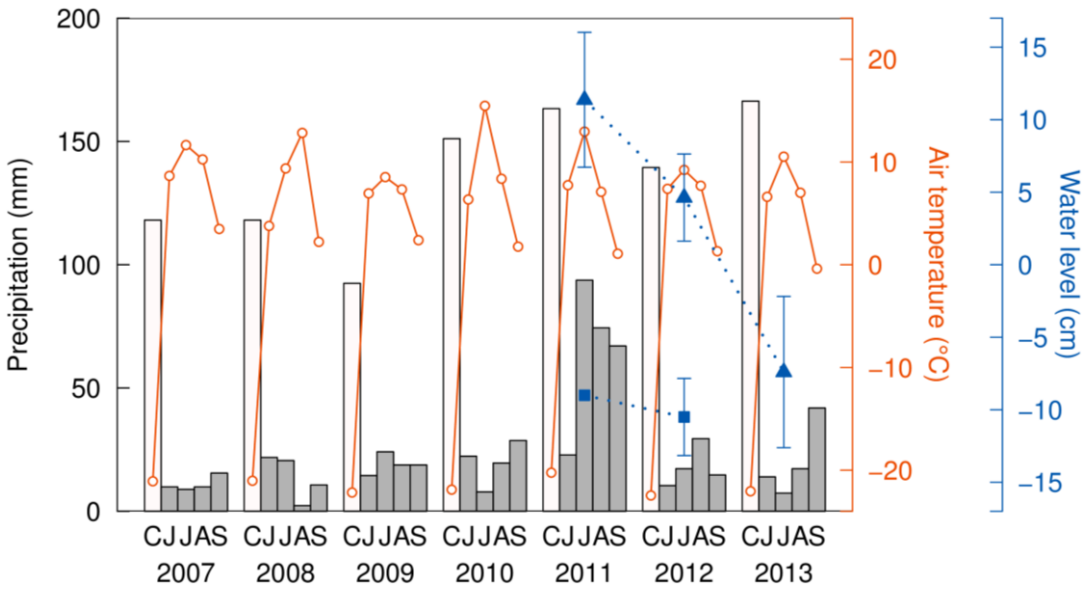

Fig. 3.1. Interannual variations in precipitation (bars) and air temperature (solid lines) observed at a weather station at Chokurdakh for the cold season with snow cover (C: total from October in the previous year to May in the current year) and the warm season (JJAS), and water level (dotted lines) measured in wet areas of sedges (triangle) and sphagnum mosses (square). Water level was very low (< −12 cm) in the wet area of sphagnum in 2013, and could not be measured. Error bars represent standard deviations. Methane flux was observed during the main summers (early July to early August) from 2009 to 2013.

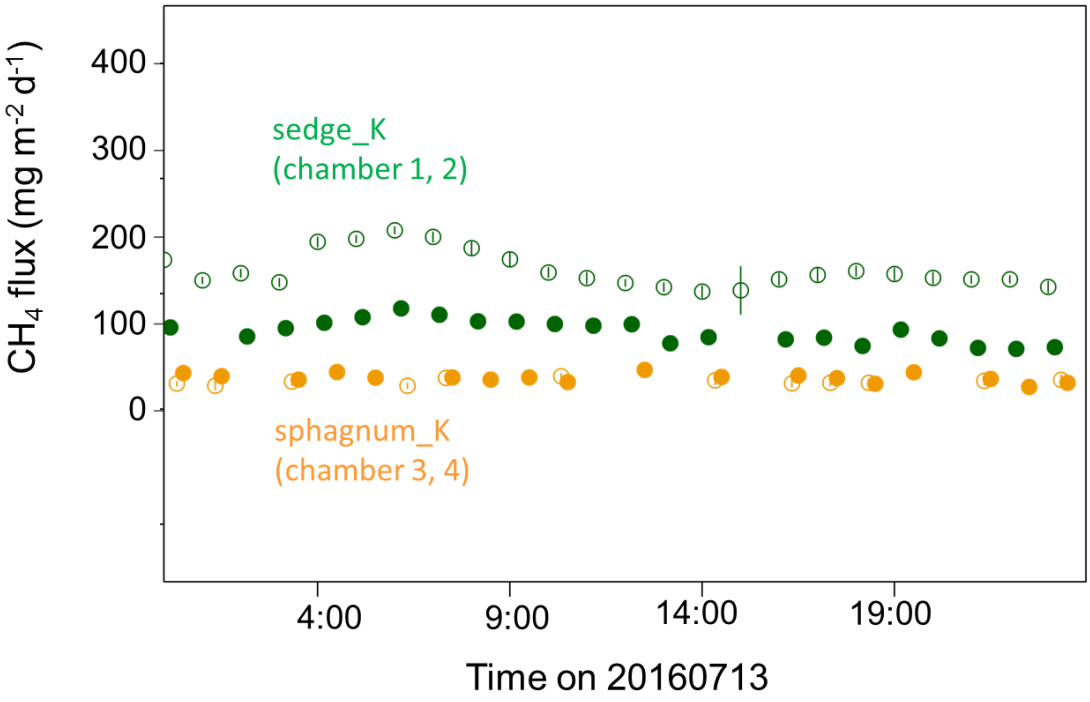

Fig. 3.2 Example of CH_4 flux observed for a whole day on 13th July 2016 in wet areas in site K by four chambers of the automatic chamber system.

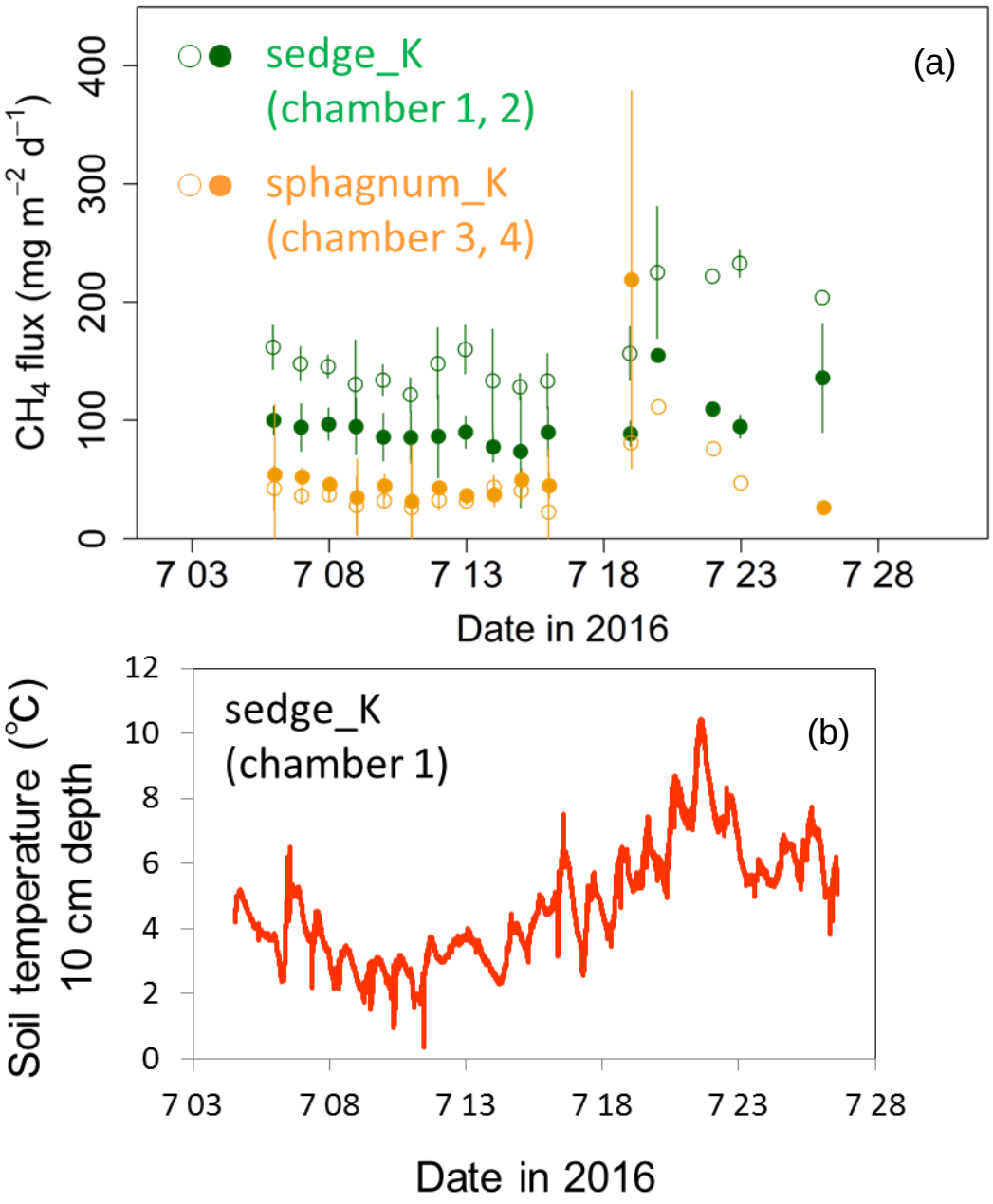

Fig. 3.3 (a) Intra-seasonal variations in CH_4 flux observed from early July to late July in 2016 in wet areas in site K by the automatic chamber system. (b) Soil temperature at 10 cm in depth in the same period.

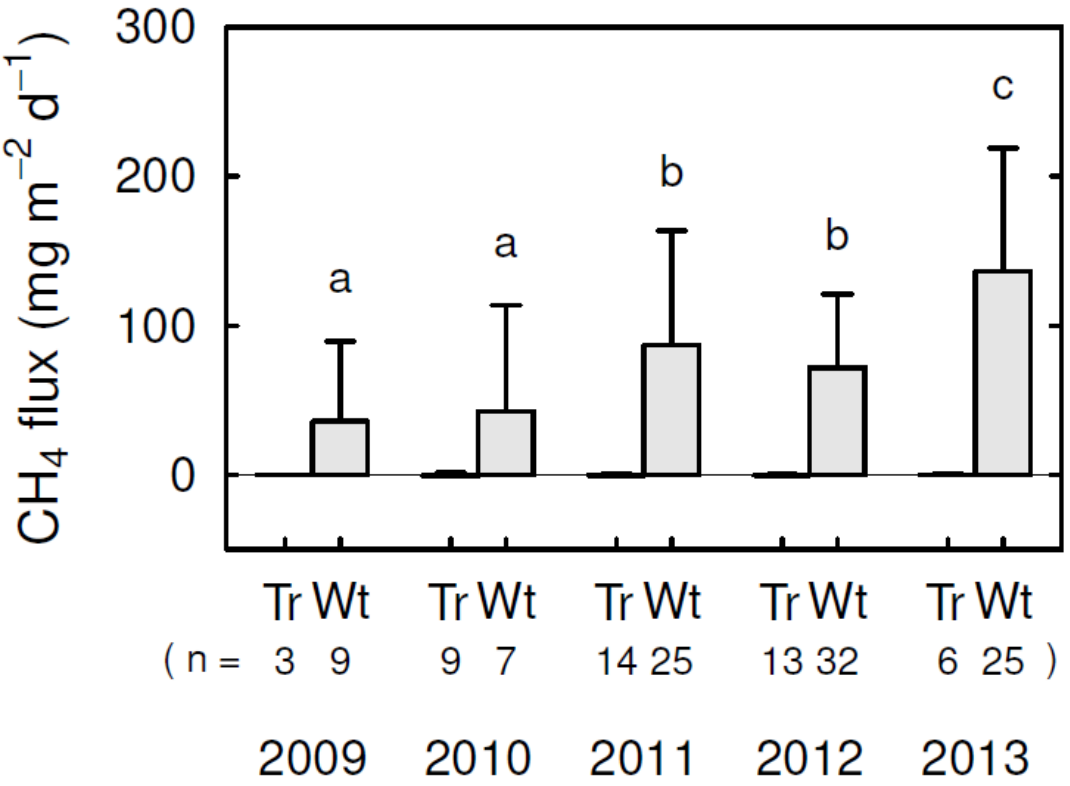

Fig. 3.4. Interannual variations in averaged CH_4 flux in tree mounds (denoted as "Tr") and wet areas ("Wt") for main summer seasons from 2009 to 2013. Replication numbers ("n") are shown for each averaged flux value, and standard deviations are represented by error bars. Different letters show statistical interannual differences in the flux values for wet areas. See Table 3.2 for flux values at respective observation points.

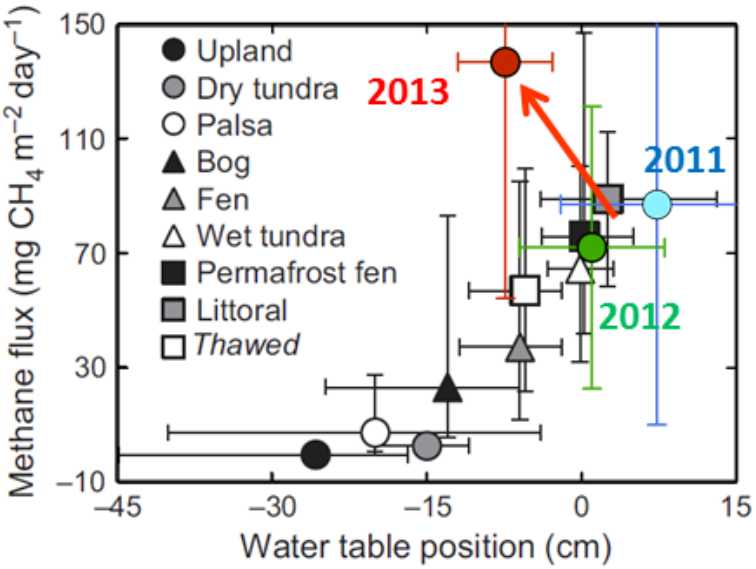

Fig. 3.5. Averaged CH_4 flux and water level observed in 2011 (wetting event), 2012, and 2013 in this study was plotted over the positive relationship between CH_4 flux and water level reported by Olefeldt et al. (2013) from metaanalysis over the circum-Arctic region. This study's data was plotted in the same scale as the figure by Olefeldt et al. (2013) and was overlaid on the figure by Olefeldt et al. (2013) using Microsoft PowerPoint 2010.

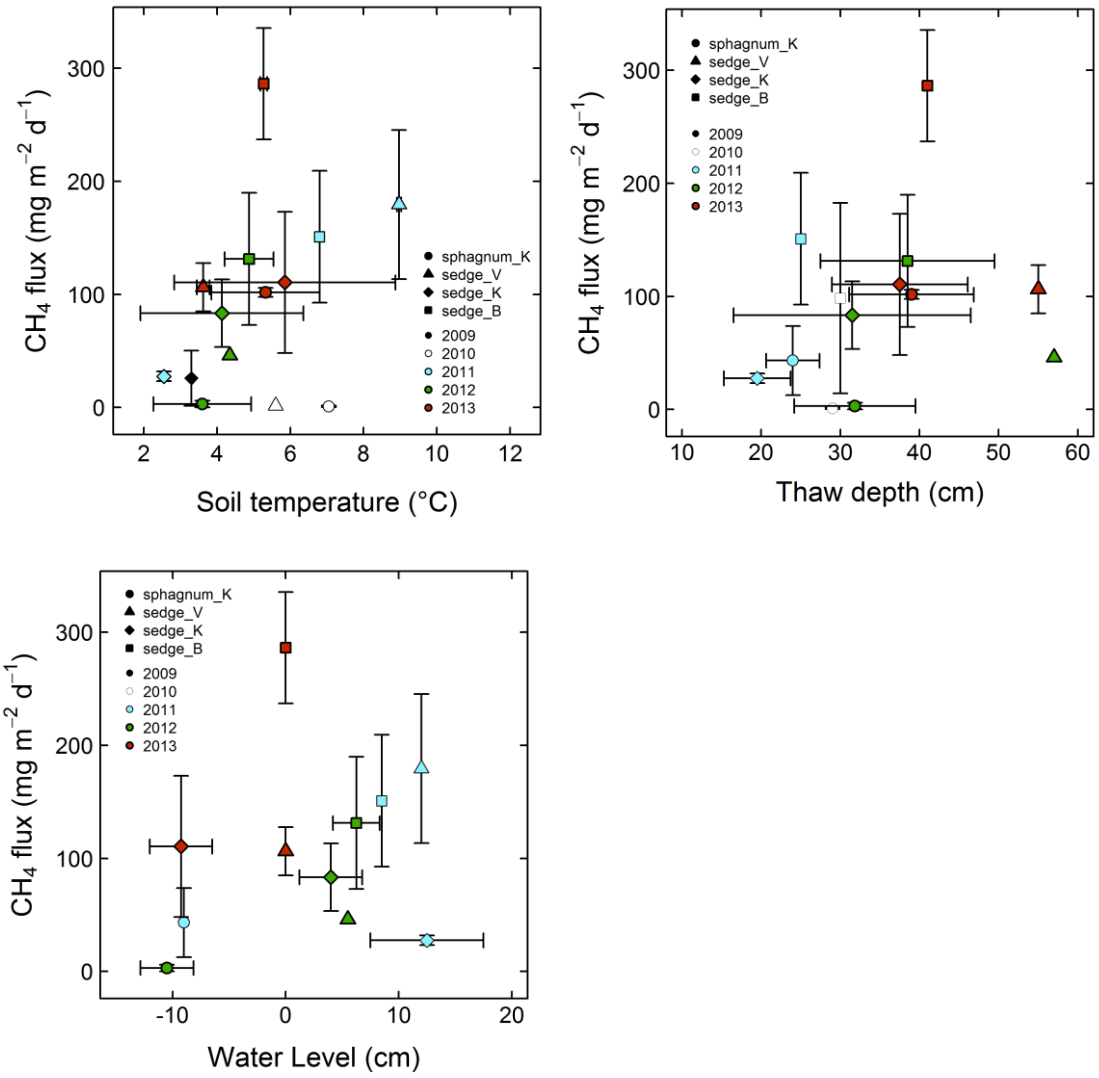

Fig. 3.6. Averaged CH_4 flux in each wet area in each year plotted against (a) soil temperature (10 cm in depth), (b) thaw depth, and (c) water level. Error bars represent standard deviations.

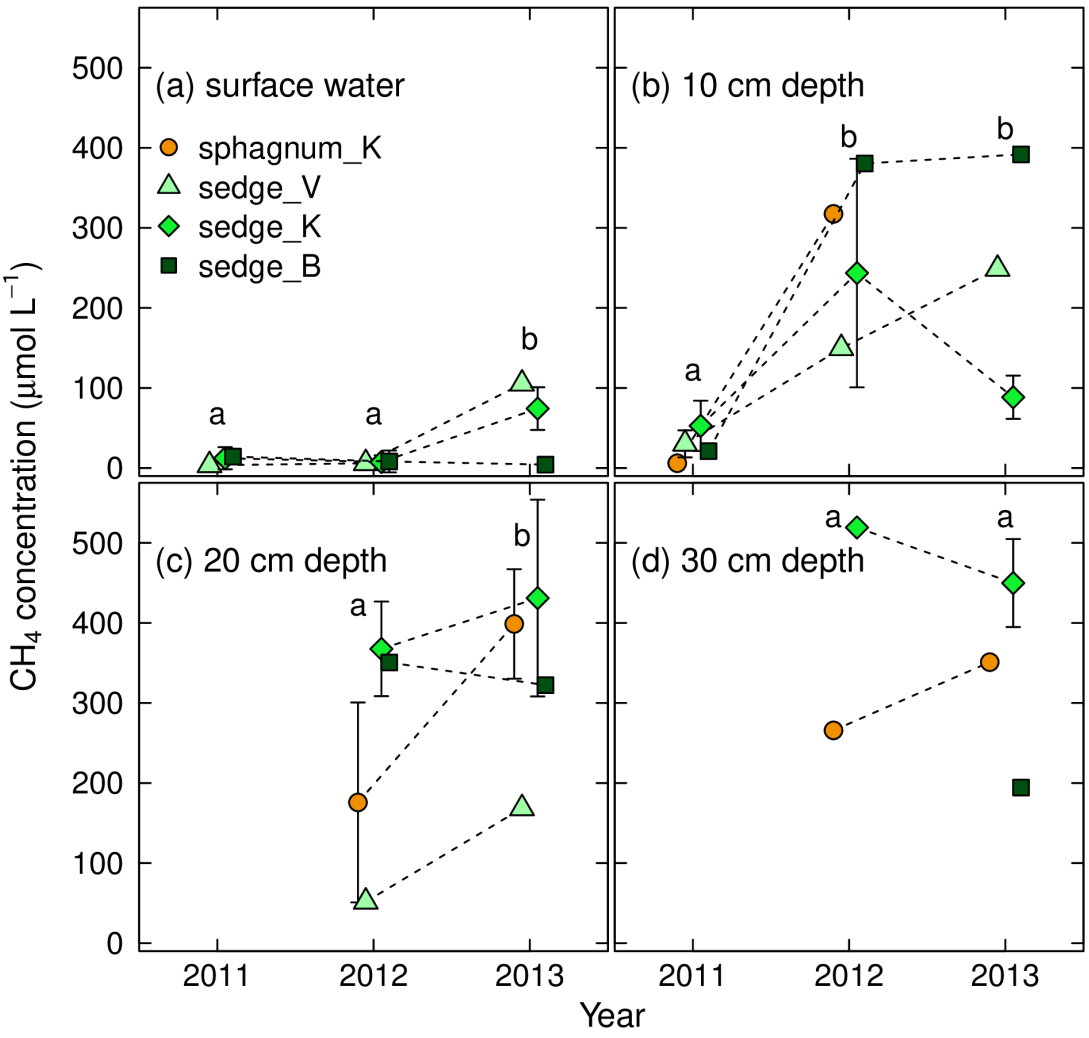

Fig. 3.7. Interannual variations in dissolved CH_4 concentration in (a) surface water and soil pore water at (b) 10 cm, (c) 20 cm, and (d) 30 cm depths in wet areas from 2011 (wetting event) to 2013. Different letters in each panel denote statistical differences among years in averaged concentration across the four wet areas ($p < 0.05$). Error bars represent standard deviations. See Table 4.1 for numerical values of dissolved CH_4 concentrations.

Chapter 4 Application of stable isotope ratios of CH_4

4.1 Objective

To investigate responses of CH_4 production and CH_4 oxidation after the wetting event in 2011, isotopic compositions of in situ dissolved CH_4 from 2011 to 2013 were assessed in this chapter. Soil incubation experiments of CH_4 production and CH_4 oxidation were also conducted to know relationship of isotope ratios of CH_4 with CH_4 production and that with CH_4 oxidation in this ecosystem. Additionally, microbial community of methanogens was analyzed by amplicon sequencing of 16S rRNA gene to discuss isotope ratios of produced CH_4 in the incubation experiment and CH_4 production pathways.

4.2 Methods of soil incubation experiments and microbial community analysis

Soil incubation experiments were conducted to estimate $\delta^{13}C$ and δD of produced CH_4 and fractionation factors of CH_4 oxidation for carbon and hydrogen isotopes. For CH_4 production experiments, surface soil was sampled in all the wet areas in Table 2.1 (sedge_V, sphagnum_K, sedge_K, and sedge_B) during summer 2013.

Samples were taken at 10 cm in depth at each sampling location. To observe vertical variations in δ values of produced CH_4 within the thaw layer, I also collected samples from two additional depths (20 and 30 cm) at sedge_K, which is a location typical of the taiga–tundra boundary region. These samples were from organic layers, except for the samples from 30 cm, which were from the top of the mineral layer.

Approximately 10 mL of soil was directly transferred into each plastic syringe (60 mL maximum capacity) along with in situ water (approximately 50 mL) to prevent the sample from being oxidized by the atmosphere. Syringes were preserved in water to ensure no leakage and were immediately preincubated for 4–8 days and then incubated in triplicate for 8 days. Preincubation and incubation temperatures were set at 5 °C. We also incubated syringes at 10 °C for samples from 10 cm in depth at sedge_K to investigate temperature dependence of δ values of produced CH_4. For each of these seven incubation treatments (sphagnum_K, sedge_V, sedge_K, and sphagnum_K, 10 cm in depth, 5 °C; sedge_K, 20 and 30 cm in depth, 5 °C; sedge_K, 10 cm in depth, 10 °C), three replicate soil samples were prepared. Water in each incubation syringe was sampled twice at the start and the end of incubation, and dissolved CH_4 was extracted using the headspace method described in Section 2.3. As a consequence,

dissolved CH_4 samples were collected in triplicate for each of the initial and final conditions of one incubation treatment.

To interpret CH_4 production in these incubation experiments, phylogenic composition of methanogens in the surface soil was additionally analyzed in 2016 using 16S rRNA gene sequencing. In July 2016, soil samples from 10 cm in depth were collected in 10 mL plastic tubes in triplicate in the same four wet areas as the anaerobic incubation experiments and kept frozen until analysis. DNA was extracted from 3 g of the soil samples as described by Ikeda et al. (2004). Extracted DNA was purified using the OneStep™ PCR Inhibitor Removal Kit (Zymo Research, California) and quantified using the Quant-iT PicoGreen dsDNA assay kit (Invitrogen, Carlsbad, California). Amplicon sequencing was conducted targeting the V3–V4 regions of 16S rRNA genes (Caporaso et al., 2011). Sequences obtained were processed through the QIIME pipeline (Caporaso et al., 2010). A representative sequence was picked from each operational taxonomic unit (OTU), and the Greengenes reference database (version 13.8) was used to assign taxonomic information and calculate the relative abundance of methanogenic archaea present.

For CH_4 oxidation, surface organic layers (0–13 cm in depth) were sampled at sphagnum_K and sedge_K in July 2012 and then kept in a refrigerator until the

experiment (6 days). These soil samples were cut into small pieces and mixed well with air. A total of 10 g (approximately 40 mL) of soil sample was transferred into plastic syringes (maximum 120 mL) in quadruplicate for each sampling location. Approximately 80 mL of air and 0.2–2 mL of 25 % CH_4 gas were added to each syringe so the total volume in each syringe was 120 mL and the headspace CH_4 concentration was 5.0×10^2–4.8×10^3 ppm. Syringes were preserved in water and incubated at 8 °C for 8 days. Headspace gas was sampled on day 0, day 4, and day 8 from each syringe into 20 mL pre-evacuated glass vials with rubber septa. Consequently, quadruplicate gas samples were collected for each location and each sampling day.

In the aerobic incubation experiments, the fractionation factors of CH_4 oxidation for carbon and hydrogen were calculated using the following Rayleigh distillation equation:

$$\ln\frac{R_t}{R_0} = \left(\frac{1}{\alpha_{ox}} - 1\right)\ln\frac{[CH_4]_t}{[CH_4]_0} \ , \quad (1)$$

where R_0 and R_t represent isotope ratios under initial conditions and at time t, respectively; α_{ox} is the fractionation factor for CH_4 oxidation (defined so that $\alpha_{ox}>1$); and $[CH_4]_0$ and $[CH_4]_t$ are CH_4 concentrations under initial conditions and at time t, respectively.

4.3 Results

4.3.1 $\delta^{13}C$ and δD of in situ dissolved CH_4

Variability in both $\delta^{13}C$ and δD of dissolved CH_4 was smaller in deeper layers, showing different patterns between $\delta^{13}C$ and δD, and across years (Fig. 4.1). The $\delta^{13}C$ of dissolved CH_4 had similarly large ranges (−68 ‰ to −40 ‰) in surface water and at 10 cm and 20 cm in depth, compared to a small range (−53 ‰ to−46 ‰) at 30 cm in depth. The δD of dissolved CH_4 was variable only in surface water (−415 ‰ to −308 ‰) and at 10 cm in depth (−417 ‰ to −341 ‰), whereas it had a constant value of around −408 ‰ at 20 and 30 cm in depth. Additionally, $\delta^{13}C$ values approached a relatively high value (approximately −50 ‰) at depth, while δD values converged to almost their lowest value. In terms of interannual variations in $\delta^{13}C$ and δD of dissolved CH_4 from 2011 to 2013, both $\delta^{13}C$ and δD values in surface soil pore water (10 cm in depth) were scattered more widely in 2011, showing standard deviations (SD) of 6.6 ‰ and 24 ‰, respectively, whereas their ranges were smaller in 2012 and 2013 (SD: 3.3 ‰ and 17 ‰ at maxima, respectively).

As shown in Fig. 4.2, convergence of $\delta^{13}C$ and δD of dissolved CH_4 is associated with dissolved CH_4 concentrations. The $\delta^{13}C$ and δD values of dissolved CH_4, including surface water and 10 cm in depth, converged at high CH_4 concentrations to

the values seen in deeper soil layers

($\delta^{13}C = -50 \pm 5$ ‰ and $\delta D = -408 \pm 5$ ‰ at >200 μmol CH_4 L^{-1}).

4.3.2 Soil incubation experiments and microbial community analysis

In the anaerobic incubation experiment, the CH_4 production rate was different among sampling locations (Fig. 4.3); the rate was higher for sedge_K and sedge_B (0.66±0.15 and 0.43±0.09 μmol day^{-1} g^{-1} (dry weight), respectively) than sedge_V and sphagnum_K (0.24±0.02 and 0.08±0.01 μmol day^{-1} g^{-1} (dry weight), respectively). At sedge_K, the sampling location tested in detail, production was more rapid for shallower soil layers among the 10, 20, and 30 cm in depth (0.66±0.15, 0.33±0.06, 0.003±0.004 μmol day^{-1} g^{-1} (dry weight), respectively; $p <$ 0.01 in Welch's ANOVA test), while no difference in the rate was found between incubation temperatures (0.66±0.15 μmol day^{-1} g^{-1} (dry weight) at 5 °C and 0.74±0.14 μmol day^{-1} g^{-1} (dry weight) at 10 °C, $p > 0.5$ in *t* test). When the CH_4 production rate was high, the $\delta^{13}C$ and δD values of produced CH_4 were less variable irrespective of sampling location, sampling depth, or incubation temperature. The $\delta^{13}C$ value of produced CH_4 at a high production rate (> 0.26 μmol day^{-1} g^{-1})(dry weight) was −55±4 ‰ ($n = 12$). Similarly, δD under rapid CH_4 production

was −410±9 ‰ (n = 12). These $\delta^{13}C$ and δD values of CH_4 obtained under rapid production were mostly comparable with the δ values of in situ dissolved CH_4 that converged in deep soil layers ($\delta^{13}C$ = −50±2 ‰ at 30 cm in depth and δD = −408±5 ‰ at 20–30 cm in depth; Fig. 4.1c and d), although $\delta^{13}C$ values in the incubation experiment were slightly lower than those in situ.

In the microbial community analysis using 16S rRNA gene sequencing (Fig. 4.4 and Table 4.3), soil with high rates of CH_4 production shown in the incubation experiment (sedge_K and sedge_B as in Fig. 4.3) had more abundant total methanogens within the detected archaea than that with slow CH_4 production rates (sphagnum_K and sedge_V). Acetoclastic methanogens in the order Methanosarcinales were higher in proportion among methanogens in sedge_K and sedge_B, where $\delta^{13}C$ values of produced CH_4 in the incubation were higher. In contrast, Methanosarcinales were fewer in proportion in sphagnum_K, where $\delta^{13}C$ of the produced CH_4 was lower.

In the CH_4 oxidation experiment, CH_4 concentration in headspace declined continuously in every sample (Fig. 4.5a). As CH_4 oxidation proceeded, both δD and $\delta^{13}C$ of the remaining CH_4 increased with a linear relationship between them (Figs. 4.5b, c and 4.6). Observed slope $\Delta(\delta D)/\Delta(\delta^{13}C)$ was 11, indicating a much larger fractionation of hydrogen than carbon, regardless of vegetation types in wet areas

(sphagnum or sedge). The hydrogen isotope fractionation factors of CH_4 oxidation calculated from the data shown in Fig. 4.6 were 1.25 and 1.16 for wet areas of sphagnum and sedge, respectively, while carbon isotope fractionations were 1.021 and 1.015, respectively.

4.4 Discussion

4.4.1 Responses of CH_4 production and oxidation processes to the wetting event supported by isotopic compositions of CH_4

In 2011, $\delta^{13}C$ and δD of dissolved CH_4 (10 cm in depth) were scattered broadly across a wide range, whereas in 2012 and 2013 the ranges were narrower and they clustered around a high $\delta^{13}C$ value (−50 ‰) and a low δD value (−408 ‰; Fig. 4.1b). Considering that δD increased much more rapidly than $\delta^{13}C$ in our oxidation experiment (Fig. 4.6), δD can be considered a sensitive indicator of CH_4 oxidation. In contrast, $\delta^{13}C$is not a good indicator because its fractionation factor of CH_4 oxidation (1.015–1.021) was similar to that of CH_4 diffusion (1.019; Chanton, 2005); thus the effects of CH_4 oxidation and diffusion cannot be discerned by $\delta^{13}C$. Additionally, δD of dissolved CH_4 (Fig. 4.1) was clearly lower in deeper layers (20 and 30 cm in depth) than in shallower layers (surface water and 10 cm in depth), which

indicates δD showed CH_4 oxidation in situ as well because shallower layers are provided with O_2 from the atmosphere and precipitation. The effect of CH_4 exchange between surface dissolved CH_4 and atmospheric CH_4 can be excluded because all the dissolved CH_4 observed in this study was highly oversaturated (> 0.3 μmol L^{-1}, Fig. 3.7) compared to the equilibrium concentration of atmospheric CH_4 (4–5 nmol L^{-1}, assuming 1–10 °C water temperature and 2 ppm atmospheric CH_4 concentration; Yamamoto et al., 1976). Thus, δD values at 10 cm in 2011 were scattered broadly compared with those in 2012 and 2013 that clustered around a low value, suggesting that CH_4 oxidation was significant in the surface soil layer during the year of the wetting event (2011). In 2012 and 2013, CH_4 oxidation became insignificant, relative to the larger pool of dissolved CH_4 (Fig. 3.7). In the CH_4 production incubation experiment, $\delta^{13}C$ and δD of produced CH_4 were less variable at higher production rates ($\delta^{13}C = -55 \pm 4$ ‰ and $\delta D = -410 \pm 9$ ‰ as in Fig. 4.3). Analogously, those of in situ dissolved CH_4 converged at a high CH_4 concentration around similar values ($\delta^{13}C = -50 \pm 5$ ‰ and $\delta D = -408 \pm 5$ ‰ in Fig. 4.2). This suggests that δ values of produced CH_4 became almost constant under rapid CH_4 production in situ and that the convergence of δ values of dissolved CH_4 observed in situ reflect rapid CH_4 production. Hence, the narrow ranges of $\delta^{13}C$ and δD values of dissolved CH_4 at 10 cm in depth

observed in 2012 and 2013 ($\delta^{13}C$ around −50 ‰ and δD around −408 ‰, Fig. 4.1b) suggest enhanced CH_4 production relative to the wetting year (2011).

The thaw depth increase after the wetting event (Table 3.1 and Section 3.4.2) cannot explain these enhanced CH_4 production and less significant CH_4 oxidation reflected in our isotopic data (Fig. 4.1b). Additionally, in the incubation experiment of CH_4 production (Fig. 4.3), the CH_4 production rate under anaerobic conditions was slower in the deeper layer, especially at 30 cm in depth (mineral soil) compared to 10 cm and 20 cm in depth (organic soil) in sedge_K. Treat et al. (2015) also reported, from a pan-Arctic synthesis of anaerobic incubations, that differences in soil types (organic/mineral) and in substrate quality along depth are important controls on CH_4 production rate. Our results from the incubations suggest that the deep layer comprised of mineral soil, where CH_4 production becomes active when thaw depth increases, is not the main region for CH_4 production.

4.4.2 Enhancement of CH_4 production and CH_4 production pathways

When CH_4 production is initiated after the onset of anoxia in rice paddy soil, it first occurs via hydrogenotrophic methanogenesis, and then by both hydrogenotrophic and acetoclastic methanogenesis, which increases CH_4 production rate (Conrad, 2007).

Afterwards, the ratio of acetoclastic to hydrogenotrophic methanogenesis can stabilize (Roy et al., 1997). Considering that this ratio is an important control on isotopic compositions of produced CH_4, stabilization of production pathways might explain the convergence in δ values of dissolved CH_4 at our study sites under high CH_4 concentration (Fig. 4.2) and the reduced variability in δ values of produced CH_4 in our experiment under rapid production conditions (Fig. 4.3). As acetoclastic methanogenesis leads to higher $\delta^{13}C$ in produced CH_4 than hydrogenotrophic methanogenesis (Sugimoto and Wada, 1993), acetoclastic methanogenesis may have been activated when dissolved CH_4 concentration or CH_4 production rate were high during our study. This interpretation is supported by the microbial community analysis (Fig. 4.4), in which acetoclastic methanogens of Methanosarcinales were more abundant in wet areas, with a higher $\delta^{13}C$ of produced CH_4 in the incubation. Therefore, the high $\delta^{13}C$ values with smaller variation observed at 10 cm in depth in 2012 and 2013 (Fig. 4.1b) suggest a greater contribution from acetoclastic methanogenesis compared to the wetting year (2011). Similar to findings from rice paddy soil (Conrad, 2007), acetoclastic methanogenesis may have experienced delayed activation after anoxic conditions began in 2011, which could also have promoted CH_4 production in 2012 and 2013.

Table 4.1. Concentration, $\delta^{13}C$, and δD of dissolved CH_4 in surface water and soil pore water averaged over each wet area and each year. Standard deviations are shown in case of $n \geq 3$. See Table 4.2 for individual concentration and δ values for 10 cm in depth in 2011 (wetting event).

Wet area	Depth	Concentration (μmol CH_4 L^{-1})			$\delta^{13}C$ (‰)			δD (‰)		
		2011	2012	2013	2011	2012	2013	2011	2012	2013
sphagnum_K	surface water	—	—	—	—	—	—	—	—	—
	10 cm	6 ± 3 (n = 6)	318 (n = 1)	—	−56 ± 9 (n = 6)	−48 (n = 1)	—	−380 ± 23 (n = 6)	−408 (n = 1)	—
	20 cm	—	176 ± 125 (n = 3)	399 ± 68 (n = 3)	—	−55 ± 10 (n = 3)	−47 ± 2 (n = 3)	—	−412 ± 4 (n = 3)	−412 ± 3 (n = 3)
	30 cm	—	266 (n = 2)	351 (n = 1)	—	−49 (n = 2)	−50 (n = 1)	—	−407 (n = 2)	−406 (n = 1)
sedge_V	surface water	3 ± 2 (n = 3)	6 (n = 2)	105 (n = 2)	−58.1 ± 0.2 (n = 3)	−56 (n = 2)	−60 (n = 2)	−378 ± 7 (n = 3)	−383 (n = 1)	−414 (n = 2)
	10 cm	30 ± 17 (n = 3)	150 (n = 1)	249 (n = 1)	−59 (n = 2)	−51 (n = 1)	−46 (n = 1)	−405 (n = 2)	−409 (n = 1)	−415 (n = 1)
	20 cm	—	52 (n = 1)	168 (n = 1)	—	−53 (n = 1)	−51 (n = 1)	—	−405 (n = 1)	−416 (n = 1)
	30 cm	—	—	—	—	—	—	—	—	—

Table 4.1 (Continued)

Wet area	Depth	Concentration (μmol CH_4 L^{-1})			$\delta^{13}C$ (‰)			δD (‰)		
		2011	2012	2013	2011	2012	2013	2011	2012	2013
sedge_K	surface water	12 ± 14 (*n* = 4)	8 ± 8 (*n* = 11)	74 ± 27 (*n* = 6)	−46 ± 4 (*n* = 4)	−51 ± 9 (*n* = 10)	−45 ± 3 (*n* = 6)	−378 ± 27 (*n* = 4)	−349 ± 30 (*n* = 4)	−388 ± 11 (*n* = 6)
	10 cm	53 ± 31 (*n* = 6)	244 ± 143 (*n* = 7)	88 ± 27 (*n* = 5)	−50 ± 1 (*n* = 6)	−52 ± 3 (*n* = 7)	−49 ± 4 (*n* = 5)	−412 ± 4 (*n* = 6)	−405 ± 21 (*n* = 7)	−392 ± 11 (*n* = 5)
	20 cm	—	368 ± 59 (*n* = 3)	431 ± 123 (*n* = 5)	—	−46 ± 1 (*n* = 3)	−54 ± 10 (*n* = 5)	—	−412 ± 1 (*n* = 3)	−407 ± 4 (*n* = 5)
	30 cm	—	519 (*n* = 2)	450 ± 55 (*n* = 3)	—	−50 (*n* = 2)	−49 ± 2 (*n* = 3)	—	−412 (*n* = 2)	−400 ± 2 (*n* = 3)
sedge_B	surface water	14 (*n* =2)	8 ± 14 (*n* = 3)	4 (*n* = 2)	−40 (*n* = 2)	−56 (*n* = 1)	−48 (*n* = 2)	−320 (*n* = 2)	−392 (*n* = 1)	−350 (*n* = 1)
	10 cm	21 (*n* = 2)	380 (*n* = 1)	392 (*n* = 1)	−47 (*n* = 2)	−53 (*n* = 1)	−51 (*n* = 1)	−360 (*n* = 2)	−405 (*n* = 1)	−404 (*n* = 1)
	20 cm	—	351 (*n* = 2)	322 (*n* = 1)	—	−54 (*n* = 2)	−53 (*n* = 1)	—	−404 (*n* = 2)	−406 (*n* = 1)
	30 cm	—	—	194 (*n* = 1)	—	—	−53 (*n* = 1)	—	—	−405 (*n* = 1)

Table 4.2. Individual values of water level, dissolved CH_4 concentration (10 cm depth), and $\delta^{13}C$ and δD of dissolved CH_4 (10 cm depth) observed in each wet area on each date in 2011 (wetting event). Duplicated data are shown in some cases. Although water level increased during July 2011, clear temporal change was not found in the δ values.

Observation point	Date in 2011	Water level (cm)	Dissolved CH_4 concentration (μmol L^{-1})	$\delta^{13}C$ of dissolved CH_4 (‰)	δD of dissolved CH_4 (‰)
sphagnum_K	Jul 17	— (< 0)	6, 8	−43, −58	−386, −394
	Jul 18	−10	2, 2	−56, −51	−363, −341
	Jul 21	−8	8, 9	−66, −65	−398, −395
sedge_V	Jul 23	10	16	−58	−409
	Jul 29	14	49, 26	−60	−401
sedge_K	Jul 11	5	–	–	–
	Jul 17	15	27, 37	−50, −52	−407, −408
	Jul 18	15	32, 35	−51, −50	−413, −414
	Jul 21	15	88, 97	−49, −49	−415, −415
sedge_B	Jul 9	6	–	–	–
	Jul 30	11	17, 26	−45, −49	−350, −369

Table 4.3 Phylogenic composition of methanogenic archaea in wet areas. Soils (organic layers) were sampled in July 2016 from 10 cm depth in the same wet areas as the CH_4 production incubation experiment in triplicate. Then, microbial communities in the samples were analyzed by amplicon sequencing of 16S rRNA gene. See Fig. 4.4 for a plot by the level of orders.

Order	Family	Genus	Relative abundance in the total sequences (%)											
			sphagnum_K (S01)	sphagnum_K (S02)	sphagnum_K (S03)	sedge_V (S07)	sedge_V (S08)	sedge_V (S09)	sedge_K (S04)	sedge_K (S05)	sedge_K (S06)	sedge_B (S10)	sedge_B (S11)	sedge_B (S12)
Methanosarcinales	Methanosarcinaceae	*Methanosarcina*	0.01	0.00	0.00	0.21	0.09	0.47	0.06	0.08	0.08	0.25	0.20	0.16
	Methanosaetaceae	*Methanosaeta*	0.00	0.00	0.00	0.00	0.13	0.06	0.74	0.80	0.93	0.82	0.91	0.78
Methanomicrobiales	Methanoregulaceae	*Candidatus* Methanoregula	0.00	0.00	0.00	0.09	0.07	0.10	0.10	0.10	0.11	0.23	0.32	0.28
	Methanospirillaceae	*Methanospirillum*	0.00	0.00	0.00	0.00	0.00	0.01	0.00	0.00	0.00	0.02	0.00	0.01
	Methanoregulaceae	Other Methanoregulaceae	0.00	0.00	0.00	0.00	0.01	0.01	0.00	0.02	0.01	0.08	0.08	0.05
Methanocellales		Methanocellales	0.00	0.00	0.00	0.00	0.00	0.00	0.07	0.07	0.09	0.00	0.00	0.00
Methanobacteriales	Methanobacteriaceae	*Methanobacterium*	0.07	0.00	0.12	0.16	0.15	0.40	1.11	1.11	1.49	0.93	0.47	0.66
E2	[Methanomassiliicoccaceae]	[Methanomassiliicoccaceae]	0.01	0.00	0.00	0.04	0.02	0.03	0.07	0.07	0.08	0.08	0.06	0.05

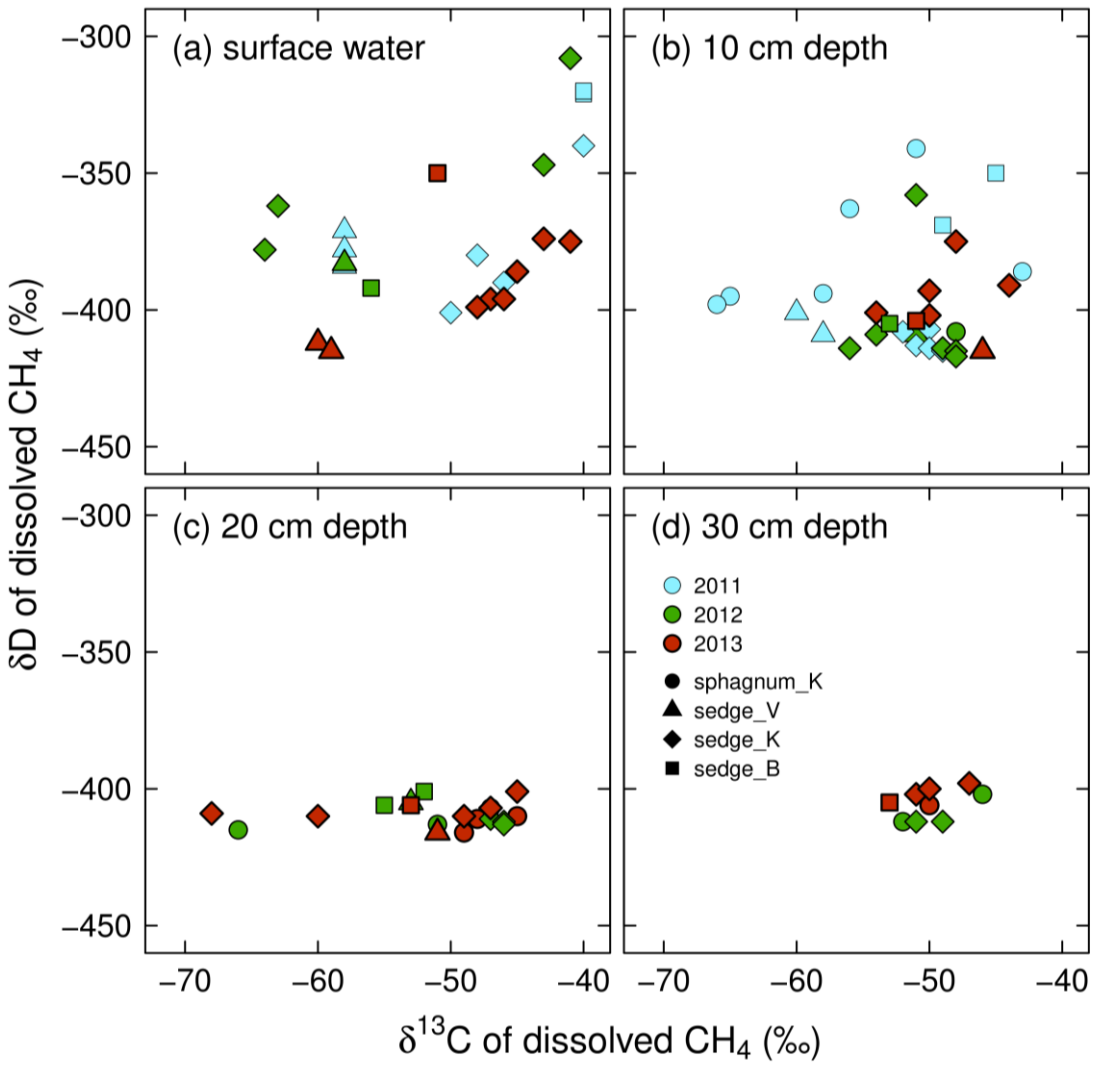

Fig. 4.1. In situ $\delta^{13}C$ versus δD of dissolved CH_4 in (a) surface water and soil pore water at (b) 10 cm depth, (c) 20 cm depth, and (d) 30 cm depth from the wet event in 2011 to 2013. Individual δ values are shown here. See Table 4.1 for averaged δ values for each observation point and each year and Table 4.2 for individual numerical δ values at 10 cm in depth in 2011.

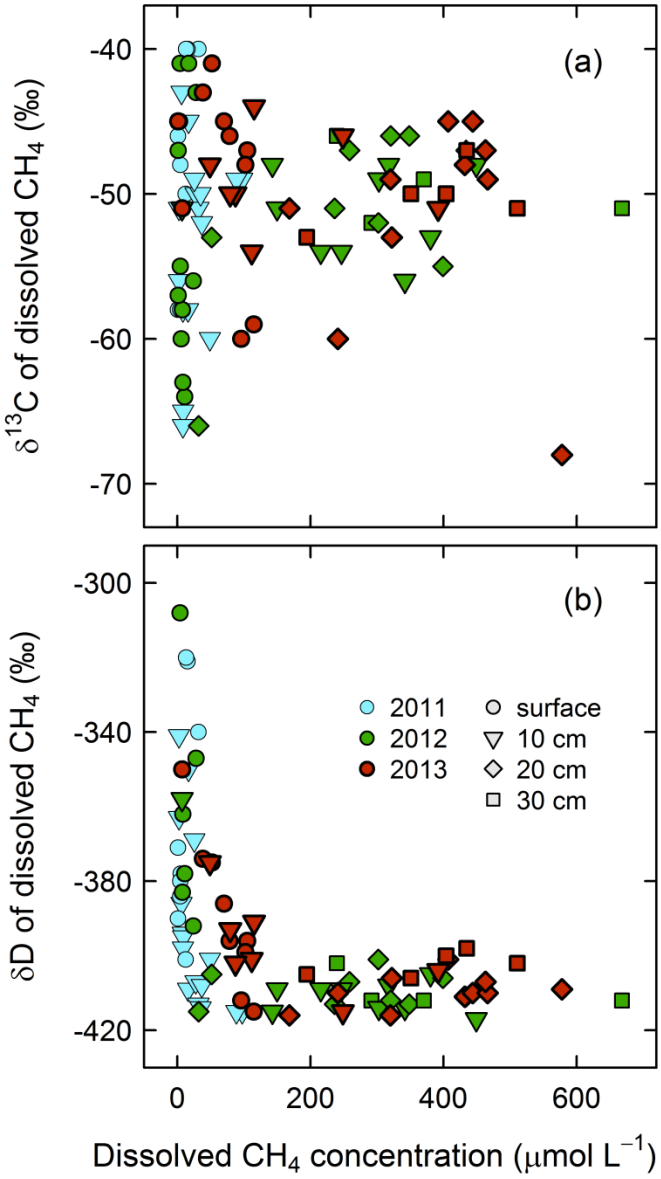

Fig. 4.2. In situ (a) $\delta^{13}C$ and (b) δD versus concentration of dissolved CH_4 at four depths (surface water, 10 cm, 20 cm, and 30 cm) in wet areas from 2011 to 2013.

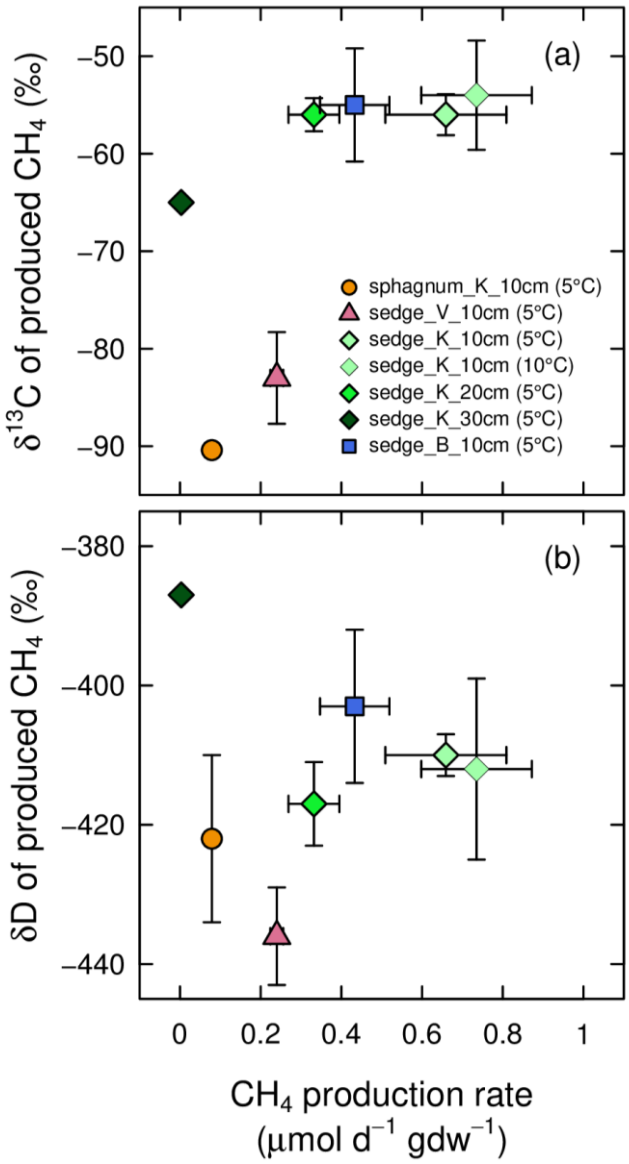

Fig. 4.3. (a) $\delta^{13}C$ and (b) δD of produced CH_4 versus CH_4 production rate in the anaerobic soil incubation experiment. Production rates are shown in micromoles of produced CH_4 per day and per weight of dry soil in grams. Soil samples were collected at four observation points (sphagnum_K, sedge_V, sedge_K, and sedge_B) at three depths (10, 20, and 30 cm) and incubated at two temperatures (5 and 10 °C). These samples contain organic layers except for those collected at 30 cm. Error bars represent standard deviations.

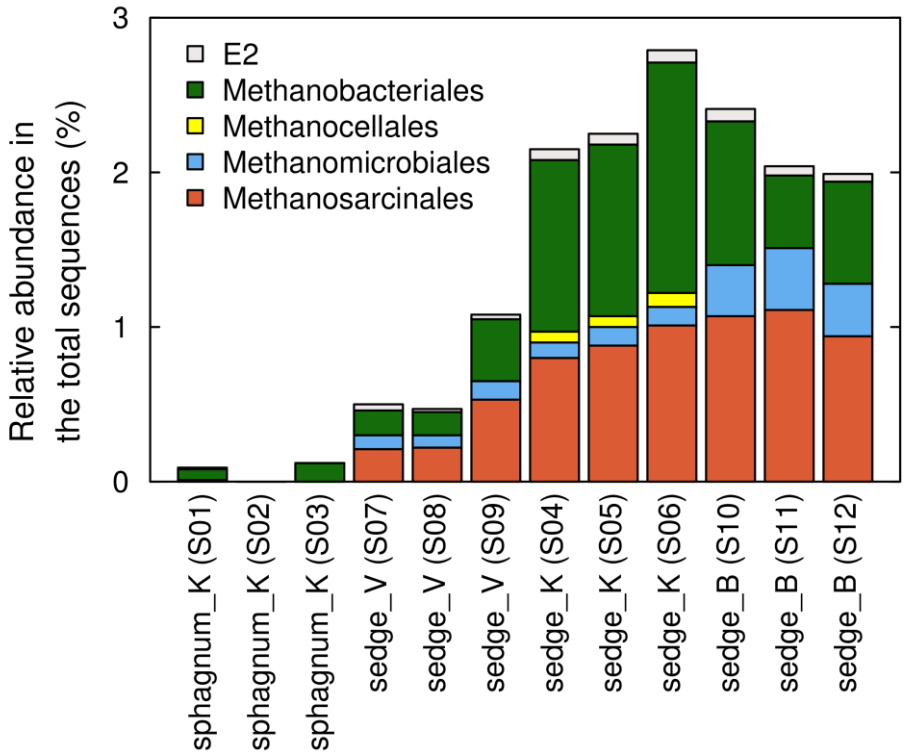

Fig. 4.4. Phylogenetic compositions of methanogenic archaea by order in wet areas. Soil samples (organic layers) were taken in triplicate from 10 cm in depth in each wet area in July 2016. See Table 4.3 for detailed results.

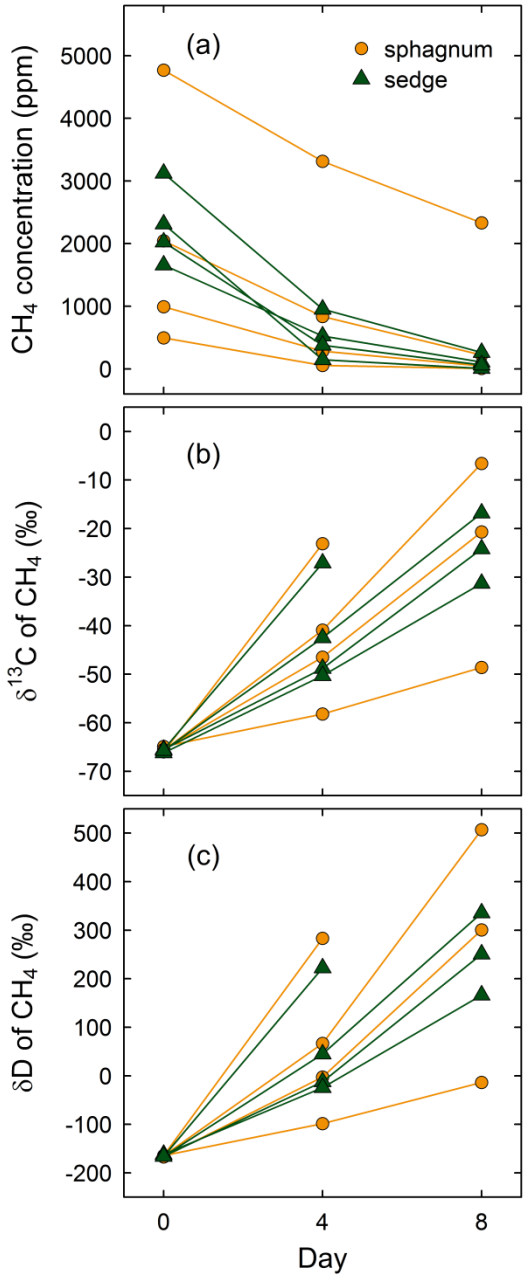

Fig. 4.5. Temporal changes in (a) concentration, (b) $\delta^{13}C$, and (c) δD of the remaining headspace CH_4 in the soil incubation experiment for CH_4 production. Surface organic layers (0–13 cm) from wet areas (sphagnum_K and sedge_K) were incubated in quadruplicate at 8 °C.

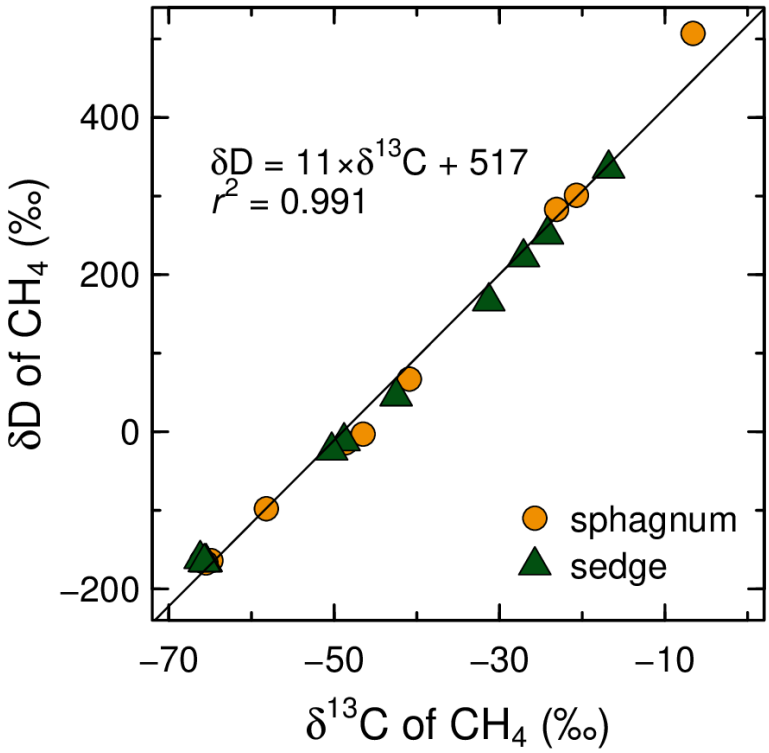

Fig. 4.6. Enrichment of D/H (CH_4) and $^{13}C/^{12}C$ (CH_4) through CH_4 oxidation during the aerobic incubation experiment of surface organic layers from wet areas of sphagnum mosses and sedges at site K. Individual δ values of the headspace CH_4 from each incubated syringe and each day are shown. Initial isotopic compositions of the headspace CH_4 were −66 ‰ to −65 ‰ for $\delta^{13}C$ and −167 ‰ to −162 ‰ for δD.

Chapter 5 General Discussion

5.1 Duration of water saturation in active layer

As seen in Fig. 4.1, isotopic compositions of dissolved CH_4 were less variable in deeper soil layer, reflecting more favorable redox conditions for CH_4 production and buildup of dissolved CH_4. In deeper active layer, water saturation conditions are assumed to be retained longer, because deep percolation is prevented by permafrost layer. Consistently, oxygen isotope ratio of water (Takano et al., unpublished) tended to show less intra-seasonal variation in deeper thaw layer. In shallower layer, $\delta^{18}O$ of water tended to increase from early July to late July, which indicates new water input because summer precipitation had higher $\delta^{18}O$ value than snowmelt water (estimated from analyses of spring snowpack; Takano et al., in preperation). In this way, duration of water saturation, which is necessary for the progress of soil reduction, can be essential for fast CH_4 production in active layer. Analogously to the vertical variation, duration of water saturation could have been important for fast CH_4 production and depressed CH_4 oxidation in 2012 and 2013 compared to 2011 (wetting event).

5.2 Inter-ecosystem comparison of lags between wetting and CH_4 emission

Multi-year effects of wetting on CH_4 flux through soil reduction processes have been previously proposed by Kumagai and Konno (1998) and Desyatkin et al. (2014) as one possible factor for explaining the increase in CH_4 flux after wetting. Kumagai and Konno (1998) reported a CH_4 flux increase at a temperate rice field in Japan 1 year after the rice field was irrigated and restored from farmland that had been drained for 8 years. Desyatkin et al. (2014) observed flux increases at a thermokarst depression in boreal eastern Siberia during the second consecutive year of flooding following large volumes of precipitation. Conversely, studies at natural wetlands in the northeastern USA (Smemo and Yavitt, 2006; Treat et al., 2007; Olson et al., 2013) and southern Canada (Moore et al., 2011) reported that interannual variations in CH_4 flux correspond with those of water level and/or precipitation in the current year. In our study area, multi-year soil reduction may be important because soil temperature is generally lower than 11 °C (10 to 30 cm in depth; Fig. 3.6 and Iwahana et al., 2014) due to a shallow active layer underlain by permafrost. Therefore, decomposition of organic matter can be slow (Treat et al., 2015), which would slowly decrease soil redox potential, allowing it to remain relatively high in the first year of wetting.

Chapter 6 Summary

At the taiga–tundra boundary on the Indigirka River lowlands, we observed an increase in CH_4 flux in wet areas following the wetting event in 2011 and a further increase in flux in 2013. Our results show interannual variations in $\delta^{13}C$ and δD of dissolved CH_4, and when compared with our incubation experiments, these variations suggest both enhancement of CH_4 production and less significance of CH_4 oxidation in 2012 and 2013 compared to 2011. This enhancement of production could be partly caused by activation of acetoclastic methanogenesis following the development of reducing soil conditions after the wetting event. Analyses of isotopic compositions of CH_4 both in situ and in incubation experiments can be combined to investigate the effects of CH_4 production and oxidation on these isotopic compositions and to clarify the relationship between CH_4 flux and wetting. In the future, measuring the $\delta^{13}C$ of dissolved CO_2 would be useful to further validate activation of acetoclastic methanogenesis (Sugimoto and Wada, 1993; McCalley et al., 2014; Itoh et al., 2015). Outside of these processes, the wetting event might have affected CH_4 flux partly via the thaw depth increase or some amount of vegetation change. It would be useful to analyze $\delta^{13}C$ and δD values of emitted CH_4 in order to assess changes in CH_4 transport (such as by increase in sedge cover) and to investigate the relationship between

dissolved CH_4 concentration and CH_4 flux in detail (Chanton, 2005).

In recent years, strong storm activity and wetting events in terrestrial ecosystems have been observed in northern regions (Iijima et al., 2016). A wetting event at the taiga–tundra boundary can switch microreliefs with large interannual variations in soil wetness conditions to significant CH_4 sources; we observed clear increases in CH_4 flux in wet areas after the wetting event. In order to predict CH_4 flux following a wetting event in a permafrost ecosystem, our results show the multi-year process of soil reduction affected by the duration of water saturation in the active layer.

Acknowledgements

I sincerely thank all the referees and staffs involved in the examination of this doctoral dissertation for the important opportunity and helpful comments.

I would like to express my deepest gratitude to Professor Atsuko Sugimoto of Hokkaido University for the precious opportunity of conducting this study, patient mentoring, and important supports for my research life. I also appreciate her observation of CH_4 flux in 2009.

I sincerely appreciate continued helpful advices and kind encouragements from Associate Professor Masanobu Yamamoto, Associate Professor Yohei Yamashita and Assistant Professor Tomohisa Irino of Hokkaido University.

I sincerely thank Mr. Shoichi Mori (Technical Division, Institute of Low Temperature Science, Hokkaido University) and Dr. Yuji Kodama (previously at Hokkaido University, currently at National Institute of Polar Research) for offering the automatic chamber system and kind supports for maintenance and trouble-shooting.

I sincerely thank Dr. Jun Murase of Nagoya University for the microbial community analyses and helpful suggestions about methane, microbiology, and pedology.

I sincerely thank Dr. Go Iwahana of Hokkaido University and University of Alaska Fairbanks for the sample analysis of CH_4 concentration in 2009, mentoring in the beginning of my fieldwork, and helpful advices about permafrost and physical environment.

I sincerely appreciate the supports for my fieldwork in the vicinity of Chokurdakh given by Dr. Trofim Maximov, Dr. Alexander Kononov, Mr. Roman Petrov, Mr. Egor Starostin, Dr. Stanislav Ksenofontov, Ms. Alexandra Alexeeva, and other members of the Institute for Biological Problems of Cryolithozone (IBPC), Siberian Branch of the Russian Academy of Sciences, and Ms. Tatiana Stryukova, Mr. Sergey Ianygin, and other staffs at the Allikhovsky Ulus Inspectorate of Nature Protection.

I also would like to appreciate technical and secretarial supports in Sugimoto Laboratory from Ms. Yumi Hoshino, Ms. Satori Nunohashi, Ms. Kanako Tanaka, Ms. Kayoko Saito, Ms. Hanae Kudo, and Dr. Masanori Ito. I truly thank Dr. Shunsuke Tei and Dr. Maochang Liang in the lab for collecting a part of the physical data and helpful information about the studied ecosystem. I truly thank Mr. Shinya Takano and Mr. Tomoki Morozumi in the lab for valuable cooperation in relation to their researches about hydrology, and about vegetation and remote sensing of the study area,

respectively. I also wish to express my appreciation to Dr. Ivan Bragin, Dr. Yumiko Miyamoto, Dr. Akihiro Ueta, Dr. Alexandra Popova, Dr. Lei Fujiyoshi, Dr. Xiaoyang Li, Dr. Fang Li, Mr. Yohei Chiba, Ms. Megumi Nakamura, Ms. Asami Kitayama, Mr. Shinichi Tanabe, Dr. Rong Fan, Mr. Ruslan Shakhmatov, Ms. Hikari Shimada, Mr. Soma Saito, Mr. Atsuki Mori, Mr. Zhou Danfeng, Mr. Shuhei Hashiguchi, Mr. Zhong Shihong, Mr. Aleksandr Nogovitsyn, and other previous and current members in Sugimoto Laboratory for helps with my fieldwork and research life.

Finally, I sincerely thank all the people who supported or encouraged this study.

References

Caporaso, J. G., Kuczynski, J., Stombaugh, J., Bittinger, K., Bushman, F. D., Costello, E. K., Fierer, N., Peña, A. G., Goodrich, J. K., Gordon, J. I., Huttley, G. A., Kelley, S. T., Knights, D., Koenig, J. E., Ley, R. E., Lozupone, C. A., McDonald, D., Muegge, B. D., Pirrung, M., Reeder, J., Sevinsky, J. R., Turnbaugh, P. J., Walters, W. A., Widmann, J., Yatsunenko, T., Zaneveld, J., and Knight, R.: QIIME allows analysis of high-throughput community sequencing data, Nat. Meth., 7, 335–336, https://doi.org/10.1038/nmeth.f.303, 2010.

Caporaso, J. G., Lauber, C. L., Walters, W. A., Berg-Lyons, D., Lozupone, C. A., Turnbaugh, P. J., Fierer, N., and Knight, R.: Global patterns of 16S rRNA diversity at a depth of millions of sequences per sample, P. Natl. Acad. Sci. USA, 108, 4516–4522, https://doi.org/10.1073/pnas.1000080107, 2011.

Chanton, J. P.: The effect of gas transport on the isotope signature of methane in wetlands, Org. Geochem., 36, 753–768, https://doi.org/10.1016/j.orggeochem.2004.10.007, 2005.

Ciais, P., Sabine, C., Bala, G., Bopp, L., Brovkin, V., Canadell, J., Chhabra, A., DeFries, R., Galloway, J., Heimann, M., Jones, C., Le Quéré, C., Myneni, R. B., Piao, S., and Thornton, P.: Carbon and other biogeochemical cycles, in: Climate change

2013: The physical science basis, Contribution of Working Group I to the Fifth Assessment Report of the Intergovernmental Panel on Climate Change, Cambridge University Press, Cambridge, UK and New York, NY, USA, 465–570, 2014.

Conrad, R.: Microbial ecology of methanogens and methanotrophs, in: Advances in Agronomy, vol. 96, Academic Press, Burlington, San Diego, USA, 1–63, 2007.

Desyatkin, A. R., Takakai, F., and Hatano, R.: Flood effect on CH_4 emission from the alas in Central Yakutia, East Siberia, Soil Sci. Plant Nutr., 60, 242–253, https://doi.org/10.1080/00380768.2014.883486, 2014.

Dlugokencky, E. J., Bruhwiler, L., White, J. W. C., Emmons, L. K., Novelli, P. C., Montzka, S. A., Masarie, K. A., Lang, P. M., Crotwell, A. M., Miller, J. B., and Gatti, L. V.: Observational constraints on recent increases in the atmospheric CH_4 burden, Geophys. Res. Lett., 36, L18803, https://doi.org/10.1029/2009GL039780, 2009.

Dutaur, L. and Verchot, L. V.: A global inventory of the soil CH_4 sink, Global Biogeochem. Cy., 21, GB4013, https://doi.org/10.1029/2006GB002734, 2007.

Flessa, H., Rodionov, A., Guggenberger, G., Fuchs, H., Magdon, P., Shibistova, O., Zrazhevskaya, G., Mikheyeva, N., Kasansky, O. A., and Blodau, C.: Landscape

controls of CH_4 fluxes in a catchment of the forest tundra ecotone in northern Siberia, Global Change Biol., 14, 2040–2056, https://doi.org/10.1111/j.1365-2486.2008.01633.x, 2008.

Iijima, Y., Nakamura, T., Park, H., Tachibana, Y., and Fedorov, A. N.: Enhancement of Arctic storm activity in relation to permafrost degradation in eastern Siberia, Int. J. Climatol., 36, 4265–4275, https://doi.org/10.1002/joc.4629, 2016.

Ikeda, S., Watanabe, K. N., Minamisawa, K., and Ytow, N.: Evaluation of Soil DNA from Arable Land in Japan Using a Modified Direct-extraction Method, Microbes Environ., 19, 301–309, https://doi.org/10.1264/jsme2.19.301, 2004.

Itoh, M., Shimamura, T., Ohte, N., and Takemon, Y.: Differences in hydrophyte life forms induce spatial heterogeneity of CH_4 production and its carbon isotopic signature in a temperate bog peatland: $\delta^{13}CH_4$ variations in hydrophyte species, J. Geophys. Res.-Biogeo., 120, 1177–1195, https://doi.org/10.1002/2014JG002881, 2015.

Iwahana, G., Takano, S., Petrov, R. E., Tei, S., Shingubara, R., Maximov, T. C., Fedorov, A. N., Desyatkin, A. R., Nikolaev, A. N., Desyatkin, R. V., and Sugimoto, A.: Geocryological characteristics of the upper permafrost in a

tundra-forest transition of the Indigirka River Valley, Russia, Polar Science, 8, 96–113, https://doi.org/10.1016/j.polar.2014.01.005, 2014.

King, G.: Responses of atmospheric methane consumption by soils to global climate change, Global Change Biol., 3, 351–362, https://doi.org/10.1046/j.1365-2486.1997.00090.x, 1997.

Kumagai, K. and Konno, Y.: Methane emissions from rice paddy fields after upland farming, Japan. J. Soil Sci. Plant Nutr., 69, 333–339, https://doi.org/10.20710/dojo.69.4_333, 1998.

Lai, D. Y. F.: Methane dynamics in northern peatlands: A review, Pedosphere, 19, 409–421, https://doi.org/10.1016/S1002-0160(09)00003-4, 2009.

Liang, M., Sugimoto, A., Tei, S., Bragin, I. V., Takano, S., Morozumi, T., Shingubara, R., Maximov, T. C., Kiyashko, S. I., Velivetskaya, T. A., and Ignatiev, A. V.: Importance of soil moisture and N availability to larch growth and distribution in the Arctic taiga-tundra boundary ecosystem, northeastern Siberia, Polar Science, 8, 327–341, https://doi.org/10.1016/j.polar.2014.07.008, 2014.

Marik, T., Fischer, H., Conen, F., and Smith, K.: Seasonal variations in stable carbon and hydrogen isotope ratios in methane from rice fields: Seasonal variations in

CH_4 isotope ratios from rice, Global Biogeochem. Cy., 16, 1094, https://doi.org/10.1029/2001GB001428, 2002.

McCalley, C. K., Woodcroft, B. J., Hodgkins, S. B., Wehr, R. A., Kim, E.-H., Mondav, R., Crill, P. M., Chanton, J. P., Rich, V. I., Tyson, G. W., and Saleska, S. R.: Methane dynamics regulated by microbial community response to permafrost thaw, Nature, 514, 478–481, https://doi.org/10.1038/nature13798, 2014.

Menne, M. J., Durre, I., Vose, R. S., Gleason, B. E., and Houston, T. G.: An overview of the Global Historical Climatology Network-Daily database, J. Atmos. Ocean. Tech., 29, 897–910, https://doi.org/10.1175/JTECH-D-11-00103.1, 2012a.

Menne, M. J., Durre, I., Korzeniewski, B., McNeal, S., Thomas, K., Yin, X., Anthony, S., Ray, R., Vose, R. S., Gleason, B. E., and Houston, T. G.: Global Historical Climatology Network – Daily (GHCN-Daily), Version 3.22, NOAA National Data Climatic Data Center, Asheville, USA, https://doi.org/10.7289/V5D21VHZ, 2012b.

Moore, T. R., De Young, A., Bubier, J. L., Humphreys, E. R., Lafleur, P. M., and Roulet, N. T.: A multi-year record of methane flux at the Mer Bleue Bog, southern Canada, Ecosystems, 14, 646–657, https://doi.org/10.1007/s10021-011-9435-9, 2011.

Morishita, T., Matsuura, Y., Kajimoto, T., Osawa, A., Zyryanova, O. A., and Prokushkin, A. S.: CH_4 and N_2O dynamics of a Larix gmelinii forest in a continuous permafrost region of central Siberia during the growing season, Polar Science, 8, 156–165, https://doi.org/10.1016/j.polar.2014.01.004, 2014.

Murase, J., Sugimoto, A., Shingubara, R., and Maximov, T. C.: Methane oxidation potential of Arctic wetland soil of a taiga-tundra ecotone in Northeastern Siberia, in: Japan Geoscience Union Meeting, 28 April–2 May 2014, Yokohama, Japan, ACG36-P16, 2014.

Myhre, G., Shindell, D., Bréon, F.-M., Collins, W., Fuglestvedt, J., Huang, J., Koch, D., Lamarque, J.-F., Lee, D., Mendoza, B., Nakajima, T., Robock, A., Stephens, G., Takemura, T., and Zhang, H.: Anthropogenic and natural radiative forcing, in: Climate change 2013: The physical science basis, Contribution of Working Group I to the Fifth Assessment Report of the Intergovernmental Panel on Climate Change, Cambridge University Press, Cambridge, UK and New York, NY, USA, 658–740, 2013.

Nakano, T., Kuniyoshi, S., and Fukuda, M.: Temporal variation in methane emission from tundra wetlands in a permafrost area, northeastern Siberia, Atmos. Environ., 34, 1205–1213, https://doi.org/10.1016/S1352-2310(99)00373-8, 2000.

Nassif, S. H. and Wilson, E. M.: The Influence of slope and rain intensity on runoff and infiltration, Hydrolog. Sci. Bull., 20, 539–553, https://doi.org/10.1080/02626667509491586, 1975.

Nisbet, E. G., Dlugokencky, E. J., and Bousquet, P.: Methane on the Rise – Again, Science, 343, 493–495, https://doi.org/10.1126/science.1247828, 2014.

Olefeldt, D., Turetsky, M. R., Crill, P. M., and McGuire, A. D.: Environmental and physical controls on northern terrestrial methane emissions across permafrost zones, Global Change Biol., 19, 589–603, https://doi.org/10.1111/gcb.12071, 2013.

Olson, D. M., Griffis, T. J., Noormets, A., Kolka, R., and Chen, J.: Interannual, seasonal, and retrospective analysis of the methane and carbon dioxide budgets of a temperate peatland, J. Geophys. Res.-Biogeo., 118, 226–238, https://doi.org/10.1002/jgrg.20031, 2013.

Parmentier, F. J. W., van Huissteden, J., van der Molen, M. K., Schaepman-Strub, G., Karsanaev, S. A., Maximov, T. C., and Dolman, A. J.: Spatial and temporal dynamics in eddy covariance observations of methane fluxes at a tundra site in northeastern Siberia, J. Geophys. Res.-Biogeo., 116, G01099, https://doi.org/10.1029/2010JG001637, 2011.

Preuss, I., Knoblauch, C., Gebert, J., and Pfeiffer, E.-M.: Improved quantification of microbial CH_4 oxidation efficiency in arctic wetland soils using carbon isotope fractionation, Biogeosciences, 10, 2539–2552, https://doi.org/10.5194/bg-10-2539-2013, 2013.

Roy, R., Klüber, H. D., and Conrad, R.: Early initiation of methane production in anoxic rice soil despite the presence of oxidants, FEMS Microbiol. Ecol., 24, 311–320, https://doi.org/10.1111/j.1574-6941.1997.tb00448.x, 1997.

Smemo, K. A. and Yavitt, J. B.: A multi-year perspective on methane cycling in a shallow peat fen in central New York State, USA, Wetlands, 26, 20–29, https://doi.org/10.1672/0277-5212(2006)26[20:AMPOMC]2.0.CO;2, 2006.

Street, L. E., Dean, J. F., Billett, M. F., Baxter, R., Dinsmore, K. J., Lessels, J. S., Subke, J.-A., Tetzlaff, D., and Wookey, P. A.: Redox dynamics in the active layer of an Arctic headwater catchment; examining the potential for transfer of dissolved methane from soils to stream water, J. Geophys. Res.-Biogeo., 121, 2776–2792, https://doi.org/10.1002/2016JG003387, 2016.

Ström, L., Falk, J. M., Skov, K., Jackowicz-Korczynski, M., Mastepanov, M., Christensen, T. R., Lund, M., and Schmidt, N. M.: Controls of spatial and

temporal variability in CH_4 flux in a high arctic fen over three years, Biogeochemistry, 125, 21–35, https://doi.org/10.1007/s10533-015-0109-0, 2015.

Sugimoto, A.: GC/GC/C/IRMS system for carbo isotope measurement of low level methane concentration, Geochem. J., 30, 195–200, https://doi.org/10.2343/geochemj.30.195, 1996.

Sugimoto, A. and Wada, E.: Carbon isotopic composition of bacterial methane in a soil incubation experiment: Contributions of acetate and CO2/H2, Geochim. Cosmochim. Ac., 57, 4015–4027, https://doi.org/10.1016/0016-7037(93)90350-6, 1993.

Sugimoto, A. and Wada, E.: Hydrogen isotopic composition of bacterial methane: CO2/H2 reduction and acetate fermentation, Geochim. Cosmochim. Ac., 59, 1329–1337, https://doi.org/10.1016/0016-7037(95)00047-4, 1995.

Teh, Y. A. and Silver, W. L.: Effects of soil structure destruction on methane production and carbon partitioning between methanogenic pathways in tropical rain forest soils, J. Geophys. Res.-Biogeo., 111, G01003, https://doi.org/10.1029/2005JG000020, 2006.

Teh, Y. A., Silver, W. L., and Conrad, M. E.: Oxygen effects on methane production and oxidation in humid tropical forest soils, Global Change Biol., 11, 1283–1297, https://doi.org/10.1111/j.1365-2486.2005.00983.x, 2005.

Treat, C. C., Bubier, J. L., Varner, R. K., and Crill, P. M.: Timescale dependence of environmental and plant-mediated controls on CH_4 flux in a temperate fen, J. Geophys. Res., 112, G01014, https://doi.org/10.1029/2006JG000210, 2007.

Treat, C. C., Natali, S. M., Ernakovich, J., Iversen, C. M., Lupascu, M., McGuire, A. D., Norby, R. J., Chowdhury, T. R., Richter, A., Šantrůčková, H., Schädel, C., Schuur, E. A. G., Sloan, V. L., Turetsky, M. R., and Waldrop, M. P.: A pan-Arctic synthesis of CH_4 and CO_2 production from anoxic soil incubations, Global Change Biol., 21, 2787–2803, https://doi.org/10.1111/gcb.12875, 2015.

van der Molen, M. K., van Huissteden, J., Parmentier, F. J. W., Petrescu, A. M. R., Dolman, A. J., Maximov, T. C., Kononov, A. V., Karsanaev, S. V., and Suzdalov, D. A.: The growing season greenhouse gas balance of a continental tundra site in the Indigirka lowlands, NE Siberia, Biogeosciences, 4, 985–1003, https://doi.org/10.5194/bg-4-985-2007, 2007.

van Huissteden, J., Maximov, T. C., and Dolman, A. J.: High methane flux from an arctic floodplain (Indigirka lowlands, eastern Siberia): Methane Flux Arctic

Floodplain Siberia, J. Geophys. Res.-Biogeo., 110, G02002, https://doi.org/10.1029/2005JG000010, 2005.

van Huissteden, J., T. C. Maximov, and A. J. Dolman: Correction to “High methane flux from an arctic floodplain (Indigirka lowlands, eastern Siberia),” J. Geophys. Res., 114, G02018, https://doi.org/10.1029/2009JG001040, 2009.

Woo, M.-K.: Permafrost hydrology, Springer, Berlin, Heidelberg, Germany, https://doi.org/10.1007/978-3-642-23462-0, 2012.

Yabuki, H., Park, H., Suzuki, R., and Ohata, T.: Baseline Meteorological Data in Siberia (BMDS) Version 5.0, 5.00, Arctic Data archive System (ADS), Japan, available at: https://ads.nipr.ac.jp/dataset/A20131107-002 (last access: 31 October 2017), 2011.

Yamamoto, S., Alcauskas, J. B., and Crozler, T. E.: Solubility of methane in distilled water and seawater, J. Chem. Eng. Data, 21, 78–80, https://doi.org/10.1021/je60068a029, 1976.